Marine Geology 279 (2011) 37–51

Contents lists available at ScienceDirect

Marine Geology

journal homepage: www.elsevier.com/locate/margeo

Reconstruction of Late-Quaternary sea- and lake-level changes in a tectonically active marginal basin using seismic stratigraphy: The Gulf of Cariaco, NE Venezuela

Maarten Van Daele [a,*], Aurélien van Welden [b,f], Jasper Moernaut [a], Christian Beck [b], Franck Audemard [c], Javier Sanchez [c], François Jouanne [b], Eduardo Carrillo [b,d], Gustavo Malavé [c], Andrés Lemus [e], Marc De Batist [a]

[a] Renard Centre of Marine Geology (RCMG), Universiteit Gent, Krijgslaan 281-S8, B-9000 Gent, Belgium
[b] Laboratoire de Géodynamique des Chaînes Alpines, UMR CNRS 5025, Université de Savoie, F-73376 Le Bourget du Lac, France
[c] Fundación Venezolana de Investigaciones Sismológicas (FUNVISIS), Prolongaçion Calle Mara, El Llanito, Caracas 1073, Venezuela
[d] Instituto de Ciencias de la Tierra, Universidad Central de Venezuela, Caracas, Venezuela
[e] Instituto Oceanográfico, Universidad de Oriente, Cumaná, Venezuela
[f] Quaternary Geology and Climate Group, Geological Survey of Norway, 7491 Trondheim, Norway

ARTICLE INFO

Article history:
Received 1 April 2010
Received in revised form 8 October 2010
Accepted 12 October 2010
Available online 18 November 2010

Communicated by D.J.W. Piper

Keywords:
Cariaco
El Pilar Fault
Late Pleistocene
seismic stratigraphy
delta
sea-level reconstruction

ABSTRACT

The Gulf of Cariaco is a marginal basin located between the Cariaco Basin and the Paria Gulf, offshore NE Venezuela, along a system of active right-lateral strike-slip faults. It is connected to the Caribbean Sea via a shallow 58-m-deep sill implying that the gulf was disconnected from the global ocean during eustatic lowstands. A dense grid of high-resolution reflection seismic profiles has been used to determine the overall tectonic structure of the gulf and to establish the seismic stratigraphy of its sedimentary infill. Six unconformity-bounded seismic–stratigraphic units were identified in the upper ~200 m of the sedimentary infill. Detailed seismic–stratigraphic and seismic-facies analysis allowed defining a series of sedimentary features that can be used as indicators of past sea or lake level in the Gulf of Cariaco: i) delta offlap breaks, ii) evaporites, and iii) erosional unconformities. Using accurate measurements of these various indicators at several locations in the gulf and a simple total subsidence model, a relative sea/lake-level history encompassing the last 130 kyr could be reconstructed. In periods of connection with the open ocean, reconstructed relative sea level correlates well with eustatic sea level. In times of disconnection, distinct lake-level fluctuations occurred, which sometimes resulted in total dessication of the gulf. Lake-level fluctuations appear to correlate with major Heinrich Events, stadials and interstadials. MIS 4, the LGM and the Younger Dryas were thus identified in the Gulf of Cariaco sedimentary record. The last reconnection to the Caribbean Sea occurred during MWP1b (around 11.5 kyr). The very good fit of the Cariaco sea/lake-level curve with the eustatic sea-level curves (both in terms of amplitude and of timing) underscores potential for future paleoclimate research of the sedimentary record contained in this marginal basin, despite its active tectonic setting.

1. Introduction

The Quaternary period has been characterized by rapid and large-scale changes in eustatic sea level, in response to variations in climate and continental ice volume (Chappell and Shackleton, 1986; Imbrie et al., 1992; Reading, 1996). In sedimentary basins, accommodation space is controlled by fluctuations in base level (i.e. eustatic sea level in marine environments, lake level in lacustrine environments), by vertical motions of the basin floor (i.e. subsidence or uplift), and by the rate of sediment accumulation (Weller, 1960). It is thus possible to reconstruct absolute base-level fluctuations if sedimentation and subsidence rates are known.

This principle has been applied previously to reconstruct Quaternary sea-level fluctuations along several passive continental margins: e.g. by using shoreface deposits in the Gulf of Lions (Jouet et al., 2006; Rabineau et al., 2005, 2006) and on the Great Barrier Reef shelf (Larcombe and Carter, 1998), and by using delta lobes and delta shorefaces on the Barcelona continental shelf (Liquete et al., 2008) and in the Eastern Mediterranean (Piper and Aksu, 1992; Skene et al., 1998), the Black Sea (Aksu et al., 2002) and the Gulf of Mexico (Anderson et al., 2004; Gardner et al., 2007). These selected studies not only deal with the reconstruction of 4th-order sea-level cycles (i.e. 100 ka cycles, e.g. Liquete et al., 2008; Rabineau et al., 2005; Skene et al., 1998), but some also recognize the imprint of 5th-order cycles (e.g. Anderson et al., 2004; Rabineau et al, 2006). However, all rely on the assumption that shoreface and delta deposits reflect in their architecture and internal stratigraphy the amplitude and timing of the glacio-eustatic variations, at least in those environments where

* Corresponding author. Tel.: +32 9 264 45 73; fax: +32 9 264 49 67.
E-mail address: maarten.vandaele@ugent.be (M. Van Daele).

0025-3227/$ – see front matter © 2010 Elsevier B.V. All rights reserved.
doi:10.1016/j.margeo.2010.10.011

the preservation potential of the sea-level indicators is assured by subsidence and burial.

A similar approach has also been applied in lacustrine environments, where lake-level fluctuations have been reconstructed from the analysis of a variety of sedimentary lake-level indicators, such as the position of delta lobes and offlap breaks, shoreline deposits, degree of sediment focusing towards the centre of the basin, etc. Gilbert (1885) was a pioneer by studying the shorelines of the Great Salt Lake in Utah. More recent examples include Lake Tanganyika and Lake Challa in Africa (McGlue et al., 2008; Moernaut et al., 2010), Lake Baikal in Russia (Urabe et al., 2004), Lake Petén Itzá in Central America (Anselmetti et al., 2006) and Lake Titicaca and Laguna Potrok Aike in South America (Anselmetti et al., 2009; D'Agostino et al., 2002).

There are a number of key prerequisites common to studies reconstructing base level: i) the depth of formation of the utilized sedimentary base-level indicator (e.g. shoreface deposit, delta lobe) should be known and should be relatively precise (i.e. small depth range), ii) subsidence history should be well constrained and well known, and iii) the preservation potential of the investigated margin or lake basin should be sufficiently high.

The Gulf of Cariaco (offshore NE Venezuela) is a marginal basin located along a system of active right-lateral strike-slip faults (a.o. the El Pilar Fault) that mark the transform boundary between the Caribbean Plate and the South American Plate (Audemard et al., 2000). As a result of this setting, the Gulf of Cariaco is affected by a series of active faults (Audemard, 2007; Audemard et al., 2000). In such a tectonically active, transtensional region, subsidence is a much more important—and more complex—factor controlling accommodation space than it is on passive margins. The Gulf of Cariaco is connected to the Caribbean Sea through a shallow, 58-m-deep sill. This implies that the Gulf of Cariaco was disconnected from the global ocean during glacio-eustatic lowstands, thus forming "Lake Cariaco". This configuration resembles that of the Marmara Sea (e.g. Beck et al., 2007) or the Gulf of Amvrakikos (western Greece) (Anastasakis et al., 2007) in the Mediterranean realm.

The marginal semi-enclosed nature of the tectonically active Gulf of Cariaco and the vicinity of the Cariaco Basin make it an ideal study area. Reconstructed sea-level changes from the Gulf of Cariaco and inferred climate variations during lacustrine periods can be compared with those recorded in the Cariaco Basin. Detection of short marine incursions could have implications for global sea-level reconstructions as well as for regional subsidence, similar to what has been observed in the Gulf of Amvrakikos (Anastasakis et al., 2007). The location of the Gulf of Cariaco at the current northern border of the Intertropical Convergence Zone (ITCZ) during northern-hemisphere summer also makes it a key area to study latitudinal shifts in the ITCZ. Also the interactions between climate variability and tectonic activity can be studied in the Gulf of Cariaco.

In this study, we used a dense grid of single-channel high-resolution sparker seismic profiles to i) determine the overall tectonic structure of the Gulf of Cariaco, ii) describe the seismic stratigraphy of the sedimentary infill, iii) propose a first-order subsidence model for the gulf, based on the analysis of key reflectors, iv) reconstruct sea- and lake-level history based on the analysis of shoreface facies, offlap breaks, erosional unconformities and key reflectors, and v) compare this sea- and lake-level curve with existing reference curves (e.g. Waelbroeck et al., 2002) in order to discuss the validity of the used assumptions and approach.

2. Regional setting

2.1. Geodynamic and geological setting

The southern coast of the Caribbean, along the northern margin of eastern South America, was already recognized as a major strike-slip fault system by Rod (1956). Later, it was identified as one of the main transform boundaries between the Caribbean Plate and the South American Plate (Minster and Jordan, 1978; Molnar and Sykes, 1969). It comprises a series of major strike-slip fault systems: the Oca-Ancón Fault, the San Sebastian Fault and the El Pilar Fault, from west to east (Fig. 1). Vignali (1977) and Vierbuchen (1978, 1984) investigated the onshore expression of the E–W-trending El Pilar Fault in detail. More recently, GPS measurements have been conducted to study the kinematics along this transform boundary (Perez et al., 2001; Weber et al., 2001). Combining the structural–geological studies and the investigations based on GPS measurements, a relative displacement between the two plates of about 2 cm/y has been deduced. 70 % of the relative displacement (1.4 cm/y) is being accommodated within a 30-km-broad deformation zone. Within the latter, the El Pilar Fault accommodates between 0.8 and 1.0 cm/y, at least (Audemard, 2000).

A major structural feature along this series of strike-slip fault systems is the Cariaco Basin (Fig. 1), a 1200-m-deep pull-apart basin, connecting the San Sebastian Fault and the El Pilar Fault (Audemard et al., 2007). Due to its anoxic conditions and biogenic sedimentation with deposition of seasonal laminations, the Cariaco Basin contains a uniquely preserved, high-resolution, sedimentary record of oceanographic and climatic history in the Caribbean region, influenced by latitudinal shifts of the ITCZ (González et al., 2008; Haug et al., 2001; Hughen et al., 2000, 2006; Lea et al., 2003; Makou et al., 2007; Peterson et al., 2000b).

Towards the east, the Cariaco Basin connects to the Gulf of Cariaco, which is ~60 km long and ~15 km wide and has a maximum water depth of 85 m. The deepest part of the gulf, known as the Guaracayal Deep (Caraballo, 1982a) (Fig. 1), was recently identified as an active, small pull-apart structure (Audemard et al., 2007) between two overlapping segments of the presently active trace of the El Pilar Fault. In the southern suburbs of Cumaná, the Caigüire Hills (Fig. 1) consist of deformed Lower Pleistocene marine clastic sediments unconformably overlain by Lower–Middle Pleistocene reefal calcareous sediments (Ascanio, 1972; Macsotay, 1976, 1977). This structure is interpreted as a push-up, or pressure ridge, formed along the main trace of the El Pilar Fault (Audemard, 2006, 2007; Audemard et al., 2000). The southeastern coastal scarp, between San Antonio del Golfo and Muelle de Cariaco (Fig. 1), represents another direct morphological expression of this active fault trace (Audemard, 2006). Several hot springs are active along the southeastern coast and along the Casanay River valley.

Several destructive earthquakes generated by the El Pilar Fault have repeatedly damaged the city of Cumaná since its construction in the 16th century (Paige, 1930). The last major event was the 1997 Cariaco earthquake ($M_w = 6.9$) (Audemard, 2006; Audemard et al., 2007; Baumbach et al., 2004), which is also recorded as a resuspension event deposit in the adjacent Cariaco Basin (Thunell et al., 1999).

The Gulf of Cariaco is bounded by the Araya Peninsula in the north and by the Eastern Interior Range in the south (Fig. 1). The Araya Peninsula, with altitudes up to ~700 m, belongs to the Coastal Range Belt (Bellizzia et al., 1976; Hackley et al., 2005) and mainly consists of Mesozoic schists with minor allochtonous metamorphosed (HP/BT) ophiolitic remnants (Campos, 1981; Stéphan et al., 1980). The Eastern Interior Range, up to 2500 m high, consists of a thick stack of deformed early Cretaceous siliciclastics and limestones.

Today, only a few small rivers drain directly into the Gulf of Cariaco. They do not represent a major source of terrigenous input (Caraballo, 1982b). However, two more important rivers, bearing large watersheds and carrying a significant sediment load, did have an outflow in the gulf during part of its Quaternary history (Fig. 1): the Manzanares and Casanay Rivers. The Manzanares River currently drains into the Caribbean westward of the city of Cumaná, but previously (it is not known when exactly) it entered the Gulf of Cariaco to the east of the city (Schmitz et al., 2006). Also the Casanay

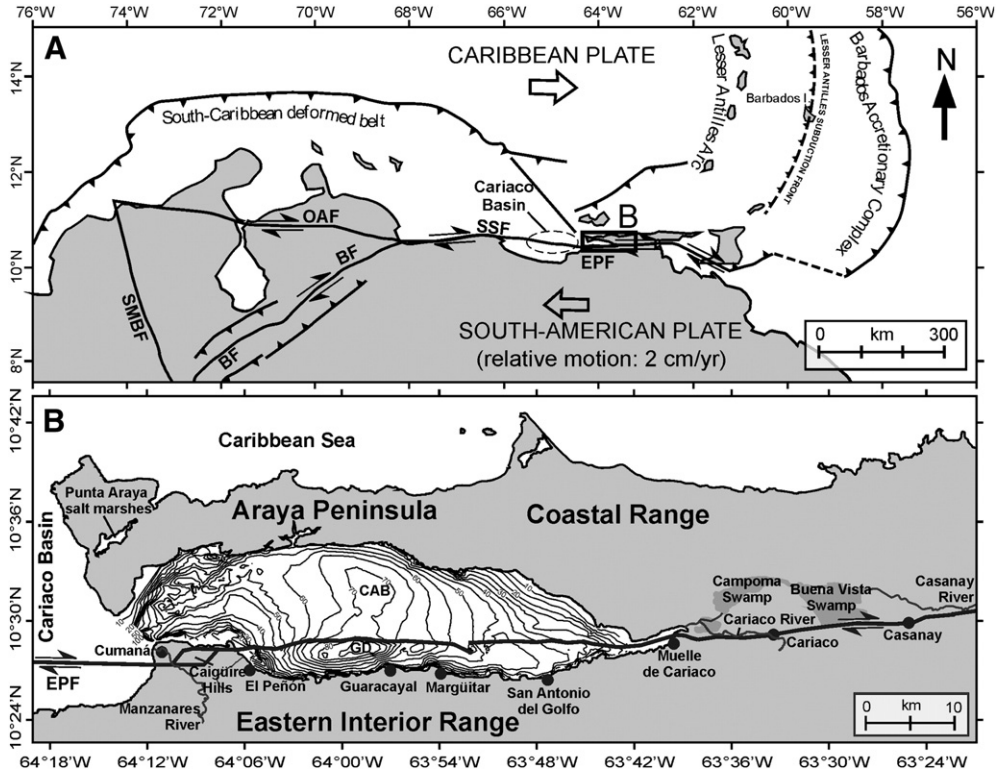

Fig. 1. A: Present-day geodynamic setting of the Gulf of Cariaco along the transform boundary between the Caribbean Plate and the South American Plate (simplified from Audemard (2007)). B: Bathymetry of the Gulf of Cariaco (from Caraballo, 1982a) and the main trace of the El Pilar Fault. Location of geographical features referred to in the text. SMBF: Santa Marta-Bucaramanga Fault; BF: Boconó Fault; CAB: Cerro Abajo Basin; EPF: El Pilar Fault; GD: Guaracayal Deep; OAF: Oca-Ancón Fault; SSF: San Sebastián Fault.

River has no more direct outflow into the southeastern termination of the gulf. It flows instead into a large shallow lake/lagoon in a flat swampy area (Fig. 1).

According to Caraballo (1982b), surface sediments in the Gulf of Cariaco are sandy in the western part of the gulf, while they consist of silty sands, sandy silts and clayey silts in the central and eastern parts. Along the southern coast, medium and fine to very fine sands are predominant. The northern coastline consists of sandy silts and fine to very fine sands in the northwest due to the stronger surge in this area (Quintero et al., 2006).

2.2. Oceanographic and climatic setting

The Gulf of Cariaco is a restricted basin (Fig. 1). The 58-m-deep sill that separates the Gulf of Cariaco from the Cariaco Basin is located north of the city of Cumaná (Fig. 1; Caraballo, 1982a). The presence of this sill implies that, during sea-level lowstands, the Gulf of Cariaco was disconnected from the world ocean and functioned as a lake. At times of disconnection, Lake Cariaco was ≤30 m deep (i.e. water depth in its central, deepest part, the Guaracayal Deep), but susceptible to climatically induced lake-level fluctuations that could have resulted in partial evaporation and even desiccation of the lake.

Current water salinity in the gulf varies between 36.24‰ and 37.66‰. Temperature of surface waters is highest between August and October (28–29 °C) and lowest in January, when it drops to 22 °C. The tidal range in the Gulf of Cariaco is about 10 to 20 cm and thus negligible (Antonius, 1980).

The depth of the wave base (about half of the wave length) in the Gulf of Cariaco can be calculated based on wind speed and effective fetch (Håkanson and Jansson, 1983; Smith and Sinclair, 1972). Currently, the average speed (in Cumaná) of the predominantly northeasterly winds varies between 2 and 5 m/s (7.6 and 18 km/h) (Quintero et al., 2006). These low values are largely due to the protection of the gulf from the trade winds by the Coastal Range.

The current total annual precipitation in Cumaná is ~250 mm/year, mean annual air temperature is 26–27 °C and annual evaporation is about 2000 mm. This results in local 'semi-desert climate with marine influence' along the southern margin of the gulf (Quintero et al., 2006). The Araya Peninsula north of the gulf is presently a desert (Bonilla et al., 1998).

3. Materials and methods

The data used in this study were collected during the "CARIELPS" expedition, which took place in January 2006 onboard of R/V Guaiqueri II, the research vessel of the Oceanographic Institute of the Universidad de Oriente in Cumaná. A dense grid of high-resolution and very-high-resolution seismic reflection profiles was shot using two different seismic systems (Fig. 2):

- 76 high-resolution seismic profiles were shot with RCMG's "Centipede" multi-electrode sparker operated at 300 or 400 J. The sparker produces a broad-spectrum seismic signal, with a mean frequency at ~1.3 kHz. A single-channel streamer with 10 hydrophones was used as receiver.
- 50 very-high-resolution pinger profiles were acquired with a 3.5 kHz GeopulseTM sub-bottom profiler.

Data were acquired at an average survey speed of 4 knots, and positioning and navigation was done by GPS. Seismic and GPS data were digitally recorded and converted to SEG-Y format with Elics™ Delph-II software. Data were subsequently interpreted using The Kingdom Suite™ software. The navigation grid (Fig. 2) was designed and dimensioned with the aim to reconstruct the 3D geometry of the sedimentary sequences and to map the different traces of the El Pilar Fault in the gulf.

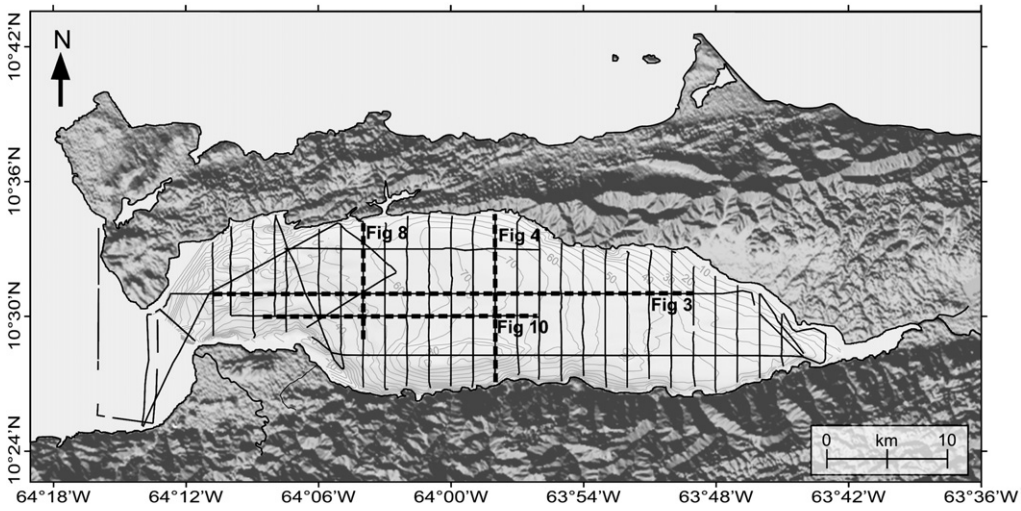

Fig. 2. Bathymetry of the Gulf of Cariaco (from Caraballo, 1982a), topography of the surrounding onshore areas (SRTM illuminated from the south) and seismic grid of the CARIELPS expedition.

4. Results

4.1. Morphology and tectonics of the Gulf of Cariaco

Five sub-areas can be identified in the Gulf of Cariaco, based on their distinct morphological and sedimentary characteristics:

i) the connection with the Cariaco Basin, at the western extremity of the gulf, is subjected to strong currents that create gullies and locally prevent sediment deposition,
ii) the Cerro Abajo Basin has a fairly flat bathymetry (Fig. 1) and is characterized by a good seismic penetration with generally south dipping parallel stratified reflectors in the centre and clinoforms towards the borders (Fig. 3),
iii) the eastern termination of the gulf (near the inflow of the Casanay River) is shallow and the units are truncated or very condensed in this area (Fig. 3),
iv) the southern part of the gulf is strongly affected by the El Pilar Fault zone, and
v) the Guaracayal Deep (85 m water depth) is confined by fault traces and the presence of shallow gas causes reduced acoustic penetration (Figs. 4 and 5).

All areas and seismic–stratigraphic units in the Gulf of Cariaco are to some degree affected by fault activity.

Faults are recognized on seismic profiles by discontinuity of seismic reflectors and hyperbolae originating from reflector terminations. The dense seismic grid (Fig. 2) enabled us to map the major faults and to gain an understanding of their geometry and history of activity. Most faults are oriented along one of two main fault directions: E–W-trending or WNW–ESE-trending faults (Fig. 5). All faults appear to be sub-vertical to vertical, even when taking into account the vertical exaggeration typically exhibited by this type of seismic data. Most of the E–W-trending faults have displaced the seafloor, while the WNW–ESE-trending faults in the centre and the eastern part of the basin are often blind faults and tend to merely flexure the upper sediments (Figs. 3 and 4). However, by measuring sediment accumulation on both sides of the faults, fault activity can be quantified. As a result we can conclude that, in addition to the known co-seismic displacement of the El Pilar Fault, both E–W- and WNW–ESE-trending faults have been active during the Late Quaternary.

In this transtensional setting and with the above-mentioned orientations with respect to the main faults in the region, the majority of these faults are expected to be strike-slip faults. The vertical offsets observed on the seismic profiles (Figs. 3 and 4) could thus be due, either to minor vertical components of predominantly strike-slip displacements, or to pure strike-slip movements affecting E–W-dipping reflectors. The very low dip angles (0.1–0.3°) observed on longitudinal profiles (E–W) (Fig. 3) favour the former interpretation. In this transtensional context, the WNW–ESE-trending vertical faults, with a combined normal and horizontal displacement, can be interpreted as Riedel faults (see Fig. 5), which are typical features in strike-slip zones (Le Pichon et al., 2001; Sylvester, 1988). The E–W-trending faults along the northern border of the Gulf of Cariaco are thus interpreted as normal faults dipping towards the south.

Considering i) the Riedel faults in the Cerro Abajo Basin, ii) the El Pilar Fault in the south, iii) the normal faults in the north and iv) the generally southward dipping reflectors, the Gulf of Cariaco can be classified as an asymmetric strike-slip basin. This type of asymmetric basins has been described by Ben-Avraham (1992) and Escalona et al. (2011), the Gulf of Elat and the Cariaco Basin being the main examples. As is typical for this type of basins, the Gulf of Cariaco is bounded by a transform fault on one side (i.e. El Pilar Fault in the south) and by predominantly normal faults on the other. According to Ben-Avraham (1992), such basins develop largely by extension normal to the transform at the same time as strike-slip motion is taking place. They explain this by a transform fault that is much weaker than the adjacent crust. This extension in a direction normal to the Principal Displacement Zone (PDZ) also explains the normal component of the Riedel faults in the Cerro Abajo Basin.

The nearly vertical Riedel faults in the Cerro Abajo Basin are dipping either to the south or to the north, with most of the faults on the northern side of the Cerro Abajo Basin dipping to the south and those in the south dipping to the north. The overall dip of the stratification is towards the south. The opposite dipping direction between the Riedel faults causes small anomalies in dip of the stratification, thereby creating the depocenter of the Cerro Abajo Basin (Fig. 5). Subsidence in the Cerro Abajo Basin is thus a combination of asymmetrical subsidence increasing towards the south (El Pilar Fault) and a subsidence component caused by normal displacement along the Riedel faults.

4.2. Seismic stratigraphy (description and interpretation)

The upper sedimentary infill of the Gulf of Cariaco, as depicted by the sparker profiles (penetration depth: <200 ms TWT or ~160 m b.s.f.), can be subdivided into 6 main seismic–stratigraphic units: i.e. Units 1 to

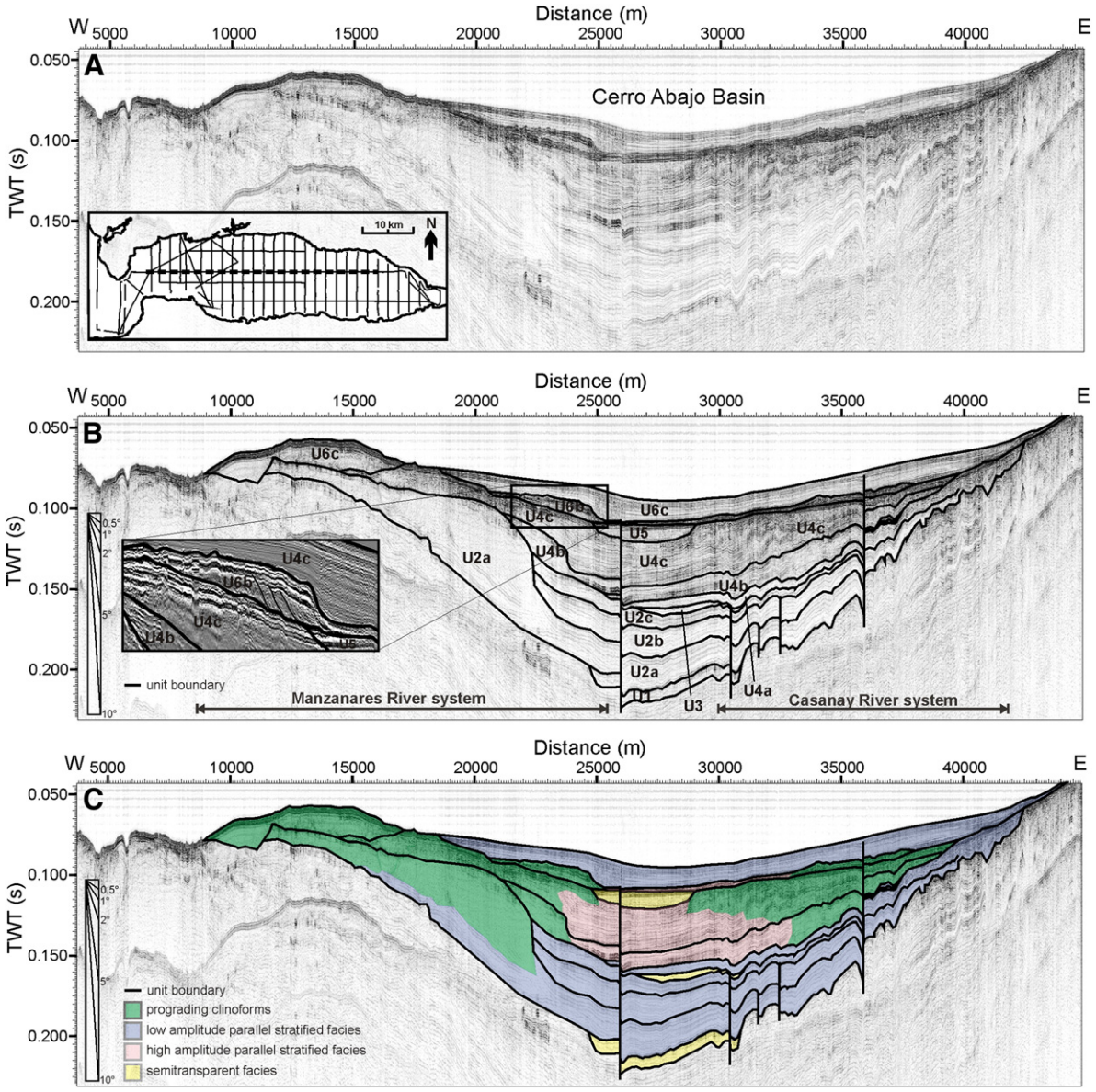

Fig. 3. Portion of longitudinal (E–W) sparker profile (sp35). A: Non-interpreted profile. B: Interpreted profile showing unit boundaries and zoom of prograding clinoforms of Unit 6b. C: Interpreted profile showing different seismic facies. Two delta-fans complexes, with several stacked clinoform units and subunits, prograde into the central Cerro Abajo Basin, i.e. a delta complex in the west associated with the Manzanares River and a delta complex in the east associated with the Casanay River. Most seismic–stratigraphic units are truncated at the seafloor in the west and are truncated or very condensed in the east. Seismic–stratigraphic units are offset by vertical faults in the central part of the basin and tend to become folded towards the east. In the westernmost part of the profile small canyons and gullies indicate currents between the Gulf of Cariaco and the adjacent Cariaco Basin.

6 (from old to young). Three of these (Units 2, 4 and 6) can be further subdivided into subunits. Each unit or subunit is delimited by an unconformity towards the margins of the basin or its correlative conformity in the centre of the basin (Figs. 3, 4, and 6). The unconformable character of unit boundaries is often very marked and present until in the centre of the Cerro Abajo Basin, while that of subunit boundaries is usually only manifested along the borders of the basin. The units are best developed and have thus been defined in the area around the Cerro Abajo Basin (Fig. 1).

Four types of seismic facies can be distinguished (Fig. 6): i) transparent to very-low-amplitude parallel stratified (i.e. semi-transparent) facies, ii) high-amplitude parallel stratified facies, iii) low-amplitude parallel stratified facies, and iv) sigmoid/upward-concave prograding clinoforms. Some of these facies types co-exist laterally within one seismic–stratigraphic unit (types ii, iii and iv), while facies type i always makes up an entire unit (Fig. 6).

4.2.1. Transparent to very-low-amplitude parallel stratified facies

Units 1, 3 and 5 are lens-shaped deposits in the centre of the Cerro Abajo Basin, with a semi-transparent facies and a strong top reflection. Unit 5 is also present in the Guaracayal Deep, but limited penetration does not allow verifying whether Units 3 and 1 are present in this deepest part of the gulf as well. Unit 3 is in all dimensions smaller than Units 1 and 5 (Figs. 3, 4, and 9). These lens-shaped bodies have a ponding configuration, filling in the irregular underlying topography and pinching out laterally. They also have a smooth upper surface. The deposits are limited to the deepest parts of the Cerro Abajo Basin and the Guaracayal Deep. The bottom reflection of Unit 5 locally exhibits clear reversed polarity (Fig. 7). Based on these geometric and geophysical characteristics, we interpret these deposits of Units 1, 3 and 5 as evaporites, formed during complete or partial dessication of the gulf. The seismic expression of these deposits is—although on a much smaller scale—very similar to that of the

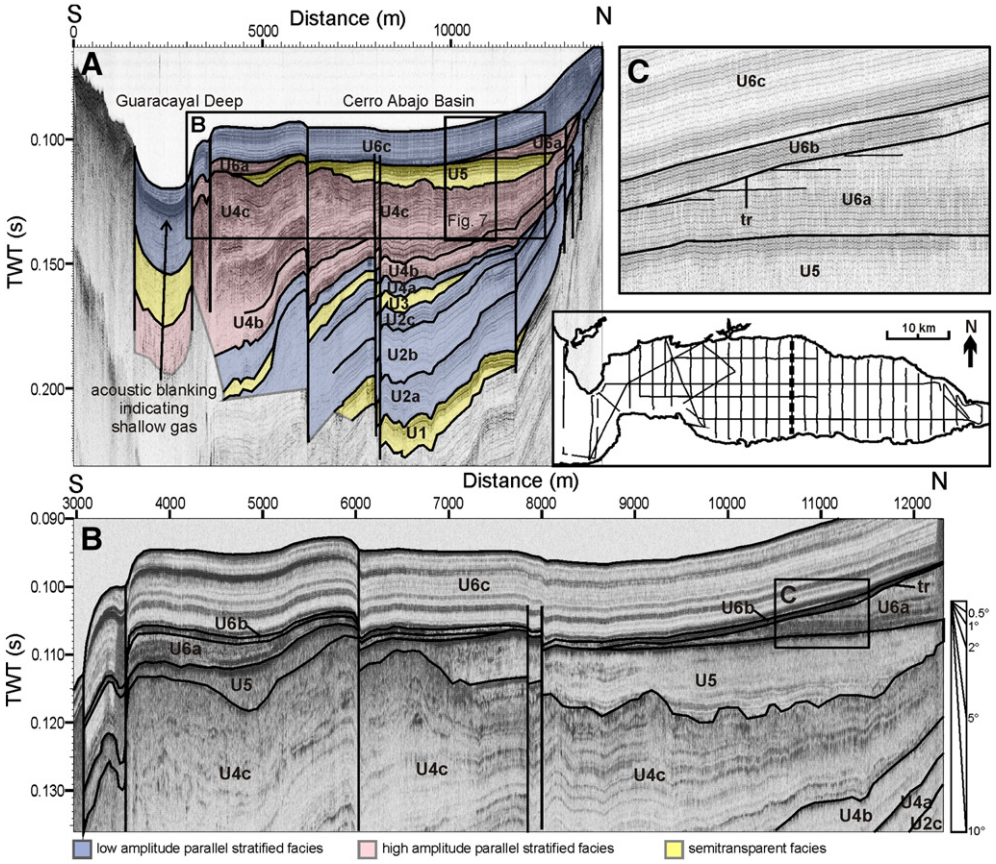

Fig. 4. Coincident 3.5 kHz (pinger) and sparker profiles across the central Gulf of Cariaco. A: Interpreted sparker profile. B: Interpreted pinger profile. C: Zoom on pinger profile showing truncation of Unit 6a. Seismic–stratigraphic units are offset by vertical faults, some of which displace the seafloor.

evaporites attributed to the Messinian Salinity Crisis in the Mediterranean (Bertoni and Cartwright, 2007). An alternative interpretation as gravitational mass-movement deposits or megaturbidites seems less likely because of the uncharacteristic (stratified) facies, the geometry (flat top; for mass-movement deposits) and the typical polarity reversal (Nurmi, 1988). Another alternative interpretation as lagoonal deposits also seems less plausible, due to the basal polarity reversal and the strong top reflection, which are not characteristic of that type of deposits.

4.2.2. Low-amplitude parallel stratified facies

In the Cerro Abajo Basin, Units 2, 4a and 6c consist of a parallel stratified facies with low-amplitude reflections. We interpret this facies as hemipelagic drape. The three subunits of Unit 2 and 4a have a

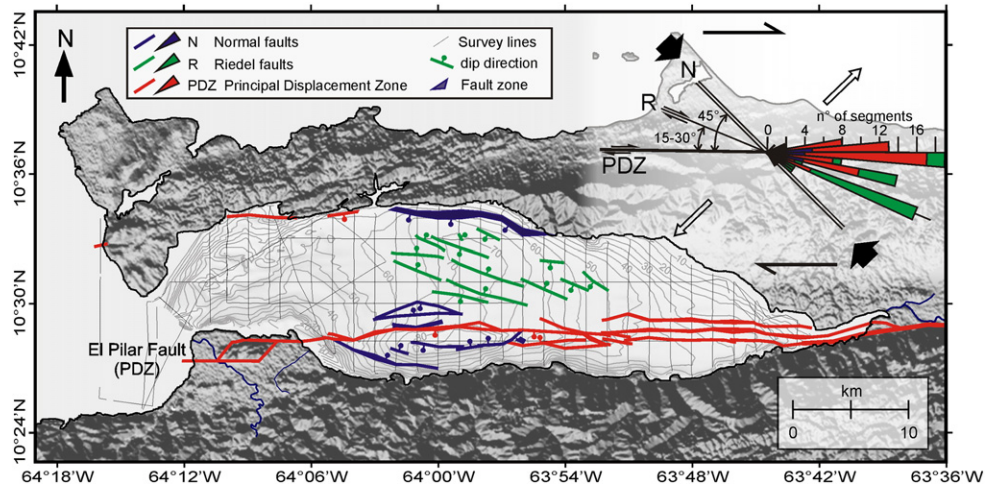

Fig. 5. Fault traces in the Gulf of Cariaco, interpreted from the reflection seismic data: El Pilar Fault along the southern shore (red) and Riedel faults in the Cerro Abajo Basin (green). Normal faults in the north and the south are indicated by blue lines. Fault directions (of each segment between 2 seismic profiles) are compared with simple shear directions along strike-slip faults proposed by Sylvester (1988).

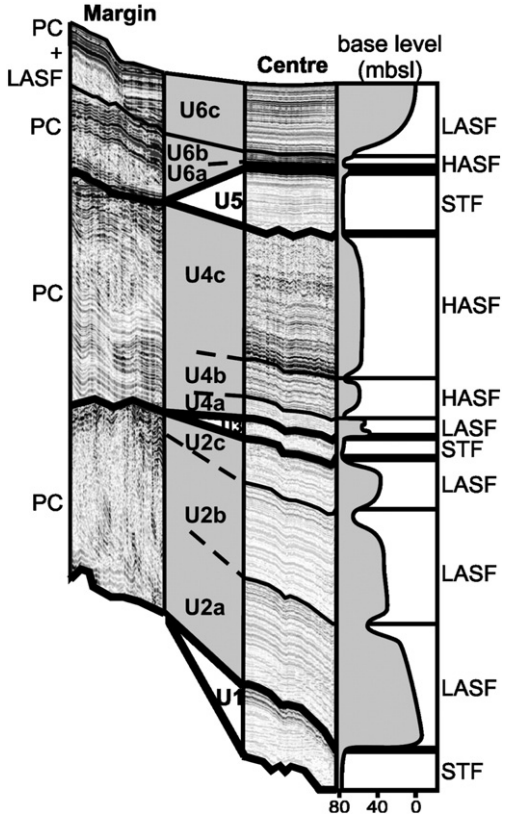

Fig. 6. Stratigraphic column of the Gulf of Cariaco illustrating the lateral and vertical distribution of the four different facies that occur in the basin: semi-transparent (STF), prograding clinoforms (PC), high-amplitude parallel (HASF) and low-amplitude parallel facies (LASF). Most units are characterized by a different facies in the centre of the basin and towards the margins. Right of the stratigraphic column the corresponding base level (green curve on Fig. 12) is presented.

high-amplitude top reflecter, grading into their correlative unconformities towards the margins of the basin (Section 4.2.5).

4.2.3. High-amplitude parallel stratified facies

Unit 4, 6a and 6b consist in the centre of the basin of high-amplitude parallel stratified facies. These draping deposits are interpreted to have been deposited under lower base-level conditions than the low-amplitude parallel stratified facies. A lower base level can lead to coarser terrestrial particles reaching the centre of the basin, therefore causing high-amplitude reflections.

4.2.4. Sigmoid/upward-concave prograding clinoforms

On both the longitudinal (E–W) and the transverse (N–S) profiles, numerous lens-shaped or mounded sediment bodies are intercalated between the parallel stratified, vertically aggrading sequences. These sediment bodies with prograding clinoforms are of various sizes (up to several km wide and long, and up to 50 ms thick) and are present in Units 2, 4 and 6. In Unit 2a, prograding clinoforms occur in the southwest and the southeast, while Units 2b and 2c have such sediment bodies in the northwest. In Units 4b and 4c the high-amplitude parallel stratified facies in the centre of the basin laterally change into several levels of prograding clinoforms, in the east and the west. Unit 6b has mounded sediment bodies with prograding clinoforms towards the western border of the Cerro Abajo Basin, while Unit 6c is characterized by both westwards and eastwards prograding clinoforms in the western part of the Gulf of Cariaco (Figs. 3, 6, 8, and 9). We interpret these bodies with prograding clinoforms as fan deltas, similar to the delta lobes described by Aksu et al. (2002) in the Black Sea and by D'Agostino et al. (2002) in Lake Titicaca.

A detailed analysis of these fan deltas allowed separating them into two main groups, representing two main sources of input: i.e. a fan delta system in the southwestern part of the Gulf of Cariaco and one in the eastern part. Although the western half of profile sp-46 (Fig. 10) displays lobes with opposite directions of apparent progradation (e.g. in Unit 6c), they belong to the same system of fan deltas. This system forms a large fan with apparent progradation over a wide range of directions (from NNW to E) (Figs. 3, 9, and 10). We interpret this system as the fan delta of the Manzanares River, formed when this river still flowed into the Gulf of Cariaco (Schmitz et al., 2006). The eastern part of profile sp-46 (Fig. 10) shows a second set of prograding lobes with less variation in progradation direction. We interpret this system as the fan delta associated with the previous course of the Casanay River. The two systems exhibit several differences (Figs. 3 and 10):

1. the Manzanares River system comprises steeper internal reflectors (i.e. the up to 6° dipping internal reflectors resemble fan-delta-type foresets) and a great variation in size and shape of delta depocentres (Figs. 8 and 10);
2. The internal reflectors of the Casanay River system are slightly folded within the area indicated on Fig. 3. Once restored, internal

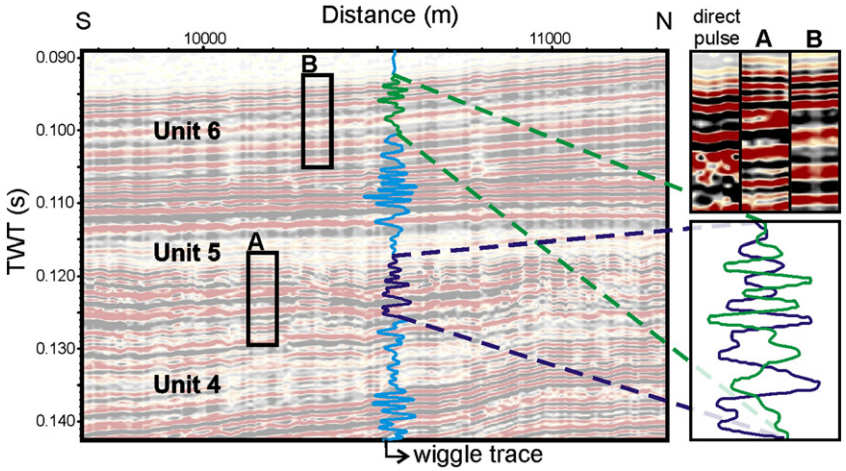

Fig. 7. Zoom on polarity reversal of the Unit 5 bottom reflections. Bottom reflections of Unit 5 (A) are compared with the seafloor reflections (B) and the direct pulse (upper right). Also the wiggle traces of the Unit 5 bottom reflections (purple) and the seafloor (green) are compared and clearly each other's opposite. Location is indicated on Fig. 4.

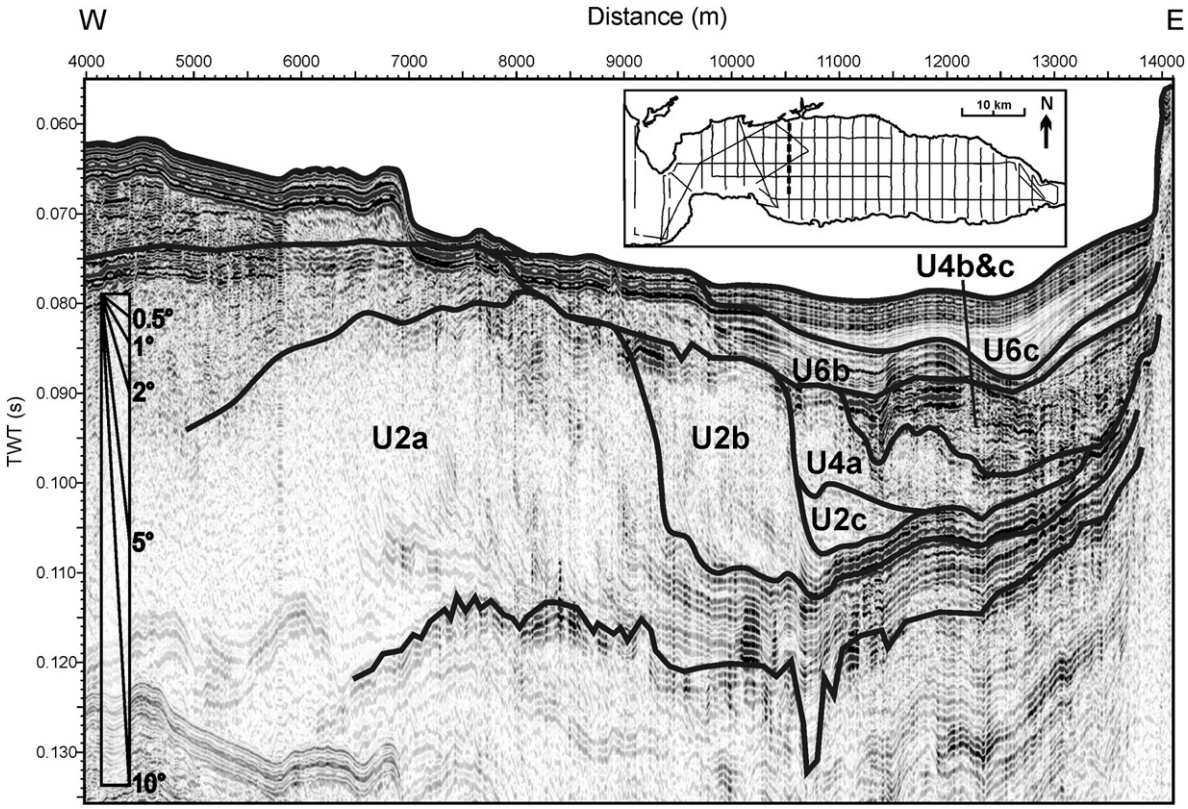

Fig. 8. Sparker profile at the western extremities of the Cerro Abajo Basin. Clear fan deltas of Units 2a, 2b and 6b can be seen. Below Units 2a and 6b (Unit 6a does not occur here) a clear erosional unconformity can be observed.

reflectors display more gentle dips, which we relate to a lower depositional energy.

The fan deltas of Unit 2 are thicker than the other ones, their prograding foreset packages spanning a height difference of more than 20 ms. This thickness is in sharp contrast with the fan deltas of Units 4 and 6, that never reach a thickness of 20 ms. Within Unit 2, the largest lobe lies in the southwest and belongs to the Manzanares system, but also in the southeast a major delta lobe is present. Several small fan deltas occur in the proximal part of the Manzanares system. It is not possible to link all of them directly to any of the units, but most of them correspond to Unit 6c (Figs. 3 and 10).

4.2.5. Erosional unconformities

The sedimentary infill of the Gulf of Cariaco is punctuated by several erosional unconformities, all of them used to define seismic units and subunits. Erosional unconformities occur at the top of Units 2a, 2b, 2c, 4a, 4b, 4c and 6a. These erosional unconformities are most pronounced at the borders of the basin and they grade into correlative conformities towards the basin centre, indicating that the unconformable character is clearly depth-controlled. However, the unconform tops of Units 2c and 4c maintain their unconform character throughout the whole basin, and are in the centre covered by the evaporites of Units 3 and 5.

5. Reconstruction of the sea- and lake-level history for the Gulf of Cariaco

5.1. Sea- and lake-level indicators

The organization of seismic units and seismic facies reveals the presence of a number of sedimentary or stratigraphic features that can be used as indicators of past sea or lake level in the Gulf of Cariaco, such as: i) evaporites, ii) delta offlap breaks, and iii) erosional unconformities.

5.1.1. Evaporites

The occurrence of evaporites in the sedimentary infill of the Gulf of Cariaco is not unlikely. The presence of the sill separating the gulf from the Cariaco Basin (i.e. at 58 m water depth) implies that during past sea-level lowstands the gulf was disconnected from the Caribbean and functioned as a lake. During those episodes, the lake level was controlled by changes in the hydrological balance and regional climate. Dry climate, with increased evaporation and/or decreased precipitation, could lead to a (partial) desiccation of the lake and to the deposition of evaporites. Previous studies have shown that during periods of low eustatic sea level, climate along the northern Venezuelan coast was much drier than during interstadials or interglacials (González et al., 2008; Hughen et al., 2004; Lea et al., 2003; Leyden, 1985; Makou et al., 2007; Peterson and Haug, 2006; Peterson et al., 2000a; Rull, 1996, 1999; Yarincik et al., 2000). Considering the present (semi)desert climate around the Gulf of Cariaco, the gulf could indeed have been desiccated during glacial periods.

The seismic units interpreted as evaporites, consist of weakly stratified, aggrading deposits. This type of evaporites is most likely formed by continuous precipitation out of oversaturated water/brine (Kendall and Harwood, 1996). These evaporites can thus be used as indicators of low lake level, related to drier climate and increased evaporation/precipitation ratio. Lake, swamp or salt level can be considered at approximately the top reflector of these evaporitic bodies (Fig. 11).

5.1.2. Delta offlap breaks

When describing the bathymetry of the Gulf of Cariaco, Caraballo (1982a) mentions the presence of shallow areas with moderate

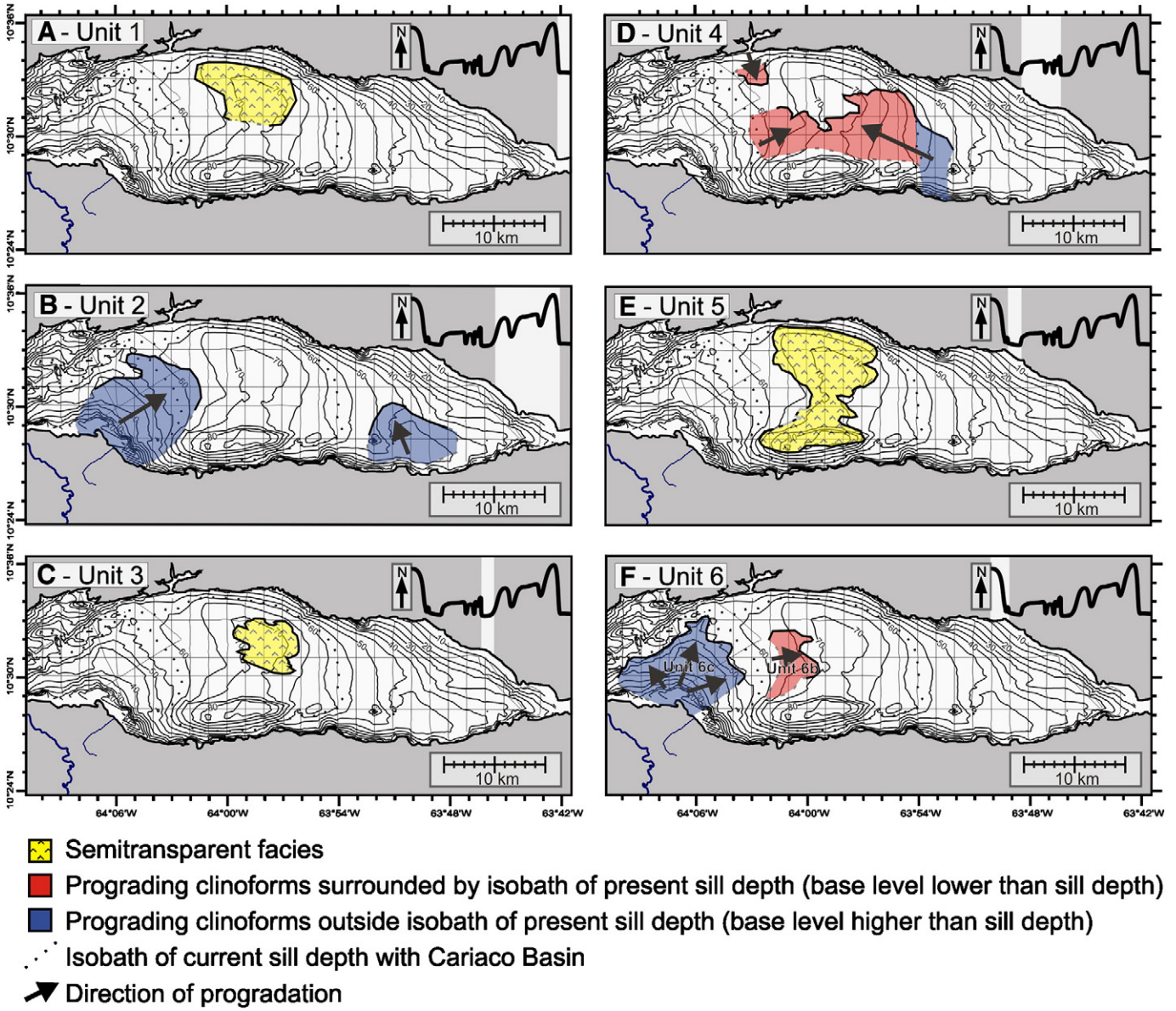

Fig. 9. Spatial distribution of prograding clinoforms and semi-transparent facies (not parallel stratified facies) in the Gulf of Cariaco, in seismic–stratigraphic Units 1 to 6. A. Unit 1: semi-transparent facies; B. Unit 2: >20 ms thick prograding clinoforms; C. Unit 3: semi-transparent facies; D. Unit 4: <20 ms thick prograding clinoforms; E. Unit 5: semi-transparent facies and F. Unit 6b (centre) and Unit 6d (west): <20 ms thick prograding clinoforms. Corresponding base level is presented in the right upper corner of each map, for absolute values see Fig. 14.

inclination and water depths between 5 and 8 m just north of the city of Cumaná and north to east of El Peñon, before an inclination increase towards the inner basin. We interpret this morphological change at 8 m water depth as the present-day offlap break.

Due to the negligible tide range and wave action, the Manzanares and Casanay River deltas can be considered as river-dominated in the present-day marine Gulf of Cariaco, and—following the same line of reasoning—also during the phases of disconnection. Offlap breaks in such deltas coincide with the fair-weather wave base (Galloway, 1975; Postma, 1990). Since the current offlap break occurs at a depth of 8 m, we can thus infer a 8 m deep wave base. Considering an effective fetch of 30 km for the dominant northeasterly tradewinds, a wind velocity of 5 m/s (ca. 18 km/h) can be calculated (see Håkanson and Jansson, 1983 for details). This value corresponds perfectly with the maximum average wind speed measured at Cumaná airport (Quintero et al., 2006). During the rainy season, the ITCZ is located at the latitude of the Gulf of Cariaco (Chiang et al., 2002), preventing tropical storms (towards the north) to affect the region. During the whole Holocene, the ITCZ is assumed to have been at a similar or slightly higher latitude as nowadays (Haug et al., 2001). We can thus infer that the Gulf of Cariaco has not been significantly struck by such tropical storms since 10 cal ky BP. According to Peterson and Haug (2006), the ITCZ shifted southwards during cold periods (glacials and stadials) and tropical storms could thus have been active in the region. However, the reduced size of the flooded basin during eustatic lowstands would induce a fetch reduction (only 10 km long, Fig. 9) resulting in a fair-weather wave base of ca. 4.5 m depth. We will thus use both end members in the base-level reconstruction: 8 m for highstands (during times of connection with Caribbean Sea) and 4.5 m for lowstands (during times of isolation of the Gulf of Cariaco) (Fig. 11).

5.1.3. Erosional unconformities

The transition between the erosional unconformities at the margins of the gulf and their correlative conformities in the centre

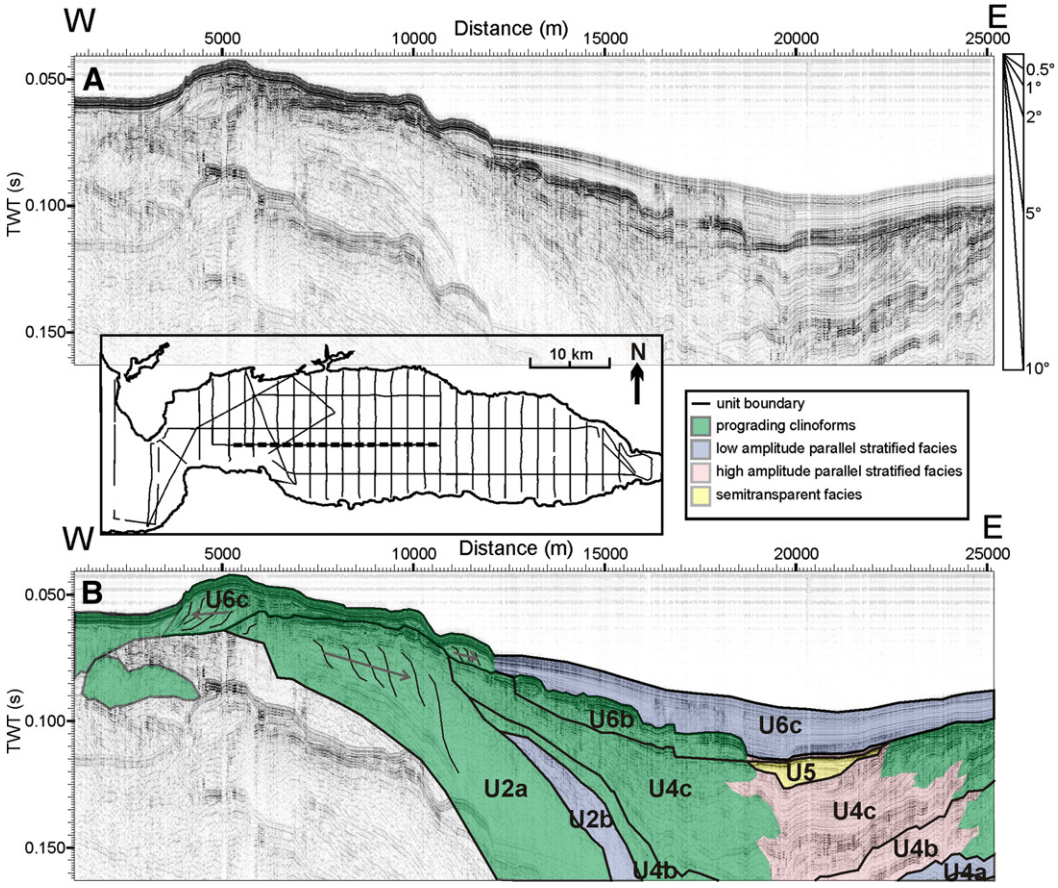

Fig. 10. Sparker profile sp46, showing the fan delta systems associated with the Manzanares (west) and Casanay (east) Rivers. Although the fan deltas in the western part all belong to the Manzanares River system, they have apparent progradation directions both to the west and the east (see also Fig. 9). This fan delta system contains fan deltas of several units: namely Units 2, 4 and 6. Of the Casanay River fan delta system only fan deltas of Unit 4 are shown in this figure. A small part of the Unit 5 evaporite is visible between Units 4 and 6.

of the gulf is strictly depth-controlled throughout the basin. We therefore surmise that this transition is predominantly determined by wave action (i.e. fair-weather wave base). During periods when sea or lake level in the gulf was lower than today and when the effective fetch was reduced, similarly as discussed above for the fan deltas, fair-weather wave base was estimated at 4.5 m (Fig. 11). These erosional unconformities can thus also be used as a (semi-quantitative) sea- or lake-level indicator.

5.2. Construction of the sea/lake-level curve

Using the above-discussed indicators (i.e. evaporites, delta offlap breaks and erosional unconformities), past relative sea- and lake levels were measured on the seismic data. Each estimate was made on several profiles, and—when possible—in different parts of the gulf, in order to increase the reliability of the method. The resulting curve (Fig. 12), plotted on a depth scale (in ms TWT) is not compensated for subsidence and compaction in its initial version.

5.3. Inferred chronology

Direct dating of the stratigraphic units is not possible due to the lack of boreholes in the gulf. Instead, we use our seismic stratigraphic and facies interpretation and the analysis of the sea/lake-level indicators and compare them with available marine and continental records to propose an indirect "working hypothesis chronology". The robustness of this hypothesis will subsequently be tested in our reconstruction. This preliminary chronology is constructed around a number of tie-points and is based on the following observations and considerations:

- Unit 5 has been interpreted as an evaporite formed during the last period of disconnection of the gulf from the world ocean (i.e. eustatic sea level below −58 m). We hence attribute it to the Last Glacial Maximum (LGM). We propose an age of 21 ka BP for the central part of the Unit 5, following Peltier and Fairbanks (2006).
- Unit 6c, the uppermost sedimentary unit in the central part of the Gulf of Cariaco, is characterized by a draping configuration and a low-amplitude parallel stratified facies, typical for fine-grained hemipelagic sedimentation. We relate this unit to the present-day marine, highstand conditions. Unit 6c would thus represent the Holocene period.
- The intervening Units 6a and 6b, which are much less widespread and less continuous than Unit 6c, were deposited in deeper-water conditions than Unit 5, but still in a significantly shallower, still lacustrine environment than Unit 6c. These units are therefore interpreted to have been deposited during the lacustrine transgression following the LGM lowstand, as also indicated by the high-amplitude seismic facies. Both units are separated by an erosional unconformity, suggesting a transgression in two pulses, separated by a lowering of the lake level.
- Based on this age model, the average deep-water sedimentation rate for Unit 6 is slightly over 1 mm/yr (assuming an acoustic velocity of 1700 m/s; Hamilton, 1978). In the nearby Cariaco Basin, where fine-grained organic sedimentation is dominating, sedimentation rates vary between 0.3 mm/yr to 1 mm/yr (Peterson et al., 2000a,b). In the

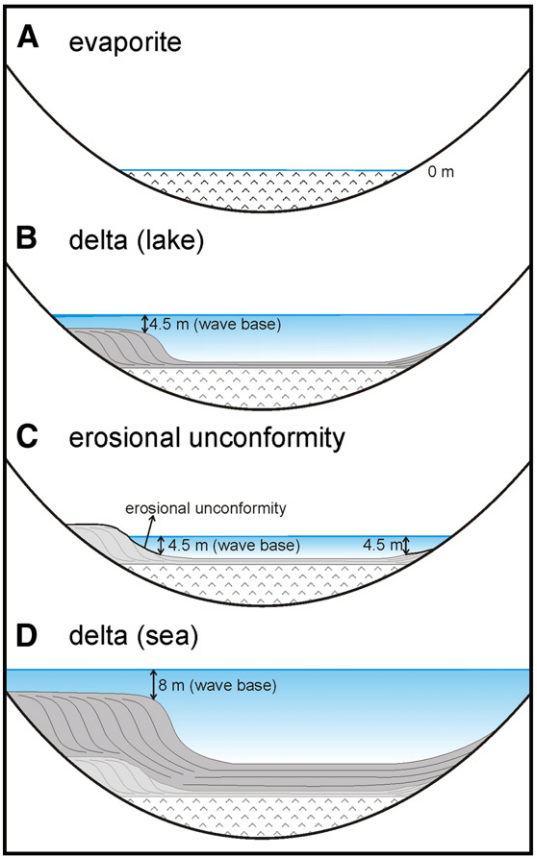

Fig. 11. Sketch of the different base-level indicators and the derived base level. A: evaporite deposit, base level at 0 m; B: fan delta in lacustrine conditions, lake level at 4.5 m above offlap break (small fetch = shallow (4.5 m) wave base); C: erosional unconformity, lake level at 4.5 m above transition between conform and unconform character; D: fan delta in marine conditions, sea level at 8 m above offlap break (equal to current offlap breaks and wave base (large fetch)).

Gulf of Cariaco, sedimentation rates are expected to be higher due to its shallow semi-enclosed and more proximal location and due to the important detrital input of the Manzanares River.

– The similarities in seismic attributes, seismic facies and distribution between Unit 5 and Units 1 and 3 lead us to interpret them as evaporitic units as well. We therefore link these units to older Late-Quaternary eustatic lowstands, when sea level was 58 m or more below its present level, and when climate was regionally much drier. Assuming a constant deep-water sedimentation rate of 1 mm/yr, Unit 1 would have been deposited between 105 and 120 ka BP. We hence attribute it to MIS 6. The intermediate evaporite of Unit 3 has a more restricted distribution in the basin (Fig. 9) and its inferred age ranges between 60 and 65 ka BP. We therefore relate it to MIS 4.
– Unit 2a represents a major, rapid rise in sea/lake-level, immediately following the lowstand of MIS 6. As the measured amplitude of the relative sea-level rise is ~120 m, we attribute Unit 2a to MIS 5e.

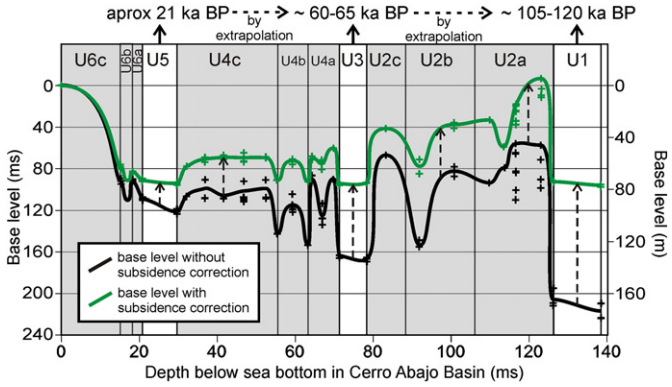

Fig. 12. Black curve: trajectory of paleo-sea/lake level—not compensated for subsidence and compaction—throughout the different seismic units in the Gulf of Cariaco. The sea/lake-level curve is obtained by plotting sea/lake-level estimations of each indicator on the vertical axis and their correlative conformity in the Cerro Abajo Basin on the horizontal axis. Green curve: sea/lake-level curve of the Gulf of Cariaco corrected for total subsidence. Data points are illustrated by black and green crosses and ages are estimated without groundtruth. Sea/lake level expressed in ms TWT relative to present-day sea level, the scale in m on the right is calculated using an arbitrary sound velocity of 1600 m/s, just to give an idea of the depth.

5.4. Subsidence model

Comparison between the reconstructed relative base-level curve and previously published eustatic sea-level data provides a first-order approach for estimating total subsidence in the basin. Inferred relative sea level of Unit 2a (attributed to MIS 5e) is located 50 m below current sea level (Fig. 12). However, according to Hearty et al. (2007), eustatic sea level during MIS 5e was 6 m above the level during MIS 1. The difference between these two values is a measure for total subsidence (i.e. a combination of flexural subsidence, tectonic subsidence and compaction of the sediments). By applying a compensation for total subsidence the descending trend of the provisional sea/lake-level curve can be corrected.

In active tectonic settings, where deformation is expressed predominantly through strike-slip faults, the characterization of the tectonic subsidence component is not straightforward. In the Gulf of Cariaco, the vertical component of the faults affecting the basin is not fully understood yet, and cannot be easily derived from the available seismic data. We therefore developed a first-order approach to infer total subsidence based on the measurable deformation of key seismic reflectors between Unit 1 and Unit 5. We hereby assumed that the evaporites attributed to MIS 6 and MIS 2 had a comparable morphology at the time of deposition, i.e. their top reflectors were horizontal and even, and they laterally merged into erosional unconformities towards the basin margin (Fig. 4). The differences in depth between these horizons are thus considered to be directly proportional to the average total subsidence at that location. In this approach, total subsidence is regarded as constant in time (i.e. between 130 and 20 ka BP), but variable in space, with higher subsidence rates in the centre than at the borders (Fig. 13).

A new sea/lake-level curve can thus be produced by applying this subsidence model on the sea/lake-level curve derived in paragraph 5.2 (Fig. 12). Time-depth conversion was done using a sound velocity of 1500 m/s for water and a mean value of 1700 m/s for sediments. Standard deviation between measurements of sea/lake-level indicators always decreases after correction (Table 1). This means that it is possible to simplify the complex interactions between flexural subsidence, tectonic subsidence, compaction and sedimentation to a simple “total subsidence” correction factor.

5.5. Comparison of the inferred sea/lake-level curve of the Gulf of Cariaco with global sea level

The reconstructed sea/lake-level curve has been compared to global sea-level curves of Waelbroeck et al. (2002) and Siddall et al. (2003) for the marine phases and to local climate reconstructions (e.g. González et al., 2008; Hughen et al., 2004) during periods of disconnection (Fig. 14). During the marine phases, the obtained sea-level curve is in very good agreement with the global sea-level data, both for what concerns the absolute sea-level heights and for the timing of the higher-frequency lowstands and highstands in between the tie-points used for our age model (i.e. correlation of Unit 1, Unit 3 and Unit 5 to isotopic stages MIS 6, MIS 4 and MIS 2, respectively).

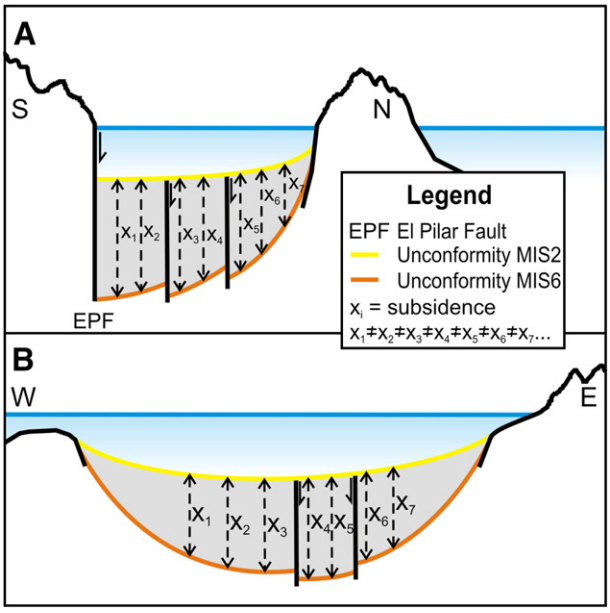

Fig. 13. Cartoon displaying subsidence model. Subsidence correction for each reflector is based on the total subsidence between two key reflectors. Subsidence correction varies depending on the location of the sea-level estimation and will be different on both sides of a fault. A: N–S profile, with in the south the El Pilar Fault (EPF) controlling most of the subsidence. B: E–W profile, with on the west the sill connecting the gulf with the Cariaco Basin.

Between MIS 6 and MIS 4, the Gulf of Cariaco curve shows three distinct highstands that closely mirror those of Waelbroeck et al. (2002). They are separated by sea-level drops, which are expressed in the sedimentary record as unconformities. Similarly, the early highstands of MIS 3 are present in both the Gulf of Cariaco record and the record of Waelbroeck et al. (2002). The close resemblance between the two records allows us to further tune our curve to those of Waelbroeck et al. (2002) and Siddall et al. (2003).

During the lacustrine phases, water level in the gulf was not driven by eustasy, but by local climate and its control on the water balance (i.e. precipitation and inflow, versus evaporation), and by the depth of the basin floor. Nevertheless, the reconstructed lake-level curve still shows a distinct—albeit apparently muted—resemblance to the eustatic curves for that period.

In more detail, we can attribute each seismic unit to a particular climatic/eustatic event (Fig. 14). Unit 1 has been correlated to MIS 6 and the subsequent highstand of MIS 5e to Unit 2a. The lower sea level of MIS 5d is represented by the upper part of Unit 2a. Unit 2b can be correlated to MIS 5c and the erosional unconformity truncating this unit to the MIS 5b lowstand, which approaches the level of the sill between the Gulf of Cariaco and the Cariaco Basin. The MIS 5a highstand can be correlated to Unit 2c.

The MIS 4 lowstand is represented by an evaporite (Unit 3) in the Gulf of Cariaco. The upper boundary of Unit 3 was tuned to the end of Heinrich Event 6 (H6), which was identified in the Cariaco Basin as a period of very dry climate (González et al., 2008).

MIS 3, which is globally characterized by a return to a higher sea level (Siddall et al., 2003; Waelbroeck et al., 2002) and, regionally by a humid and moist climate (Rull, 1999), can be correlated with Unit 4. Reconstructed base level for Unit 4 hovers around the height of the sill, implying that the environment was mostly lacustrine with some marine connections. The two unconformities separating the three subunits of Unit 4 are interpreted to have formed during a period of disconnection. They appear to be roughly coeval with Heinrich Events 5 (H5) and 5a (H5a) (Fig. 14). According to González et al. (2008), these Heinrich Events are expressed as extreme stadials in the adjacent Cariaco Basin, characterized by dry climate conditions. However, to strengthen these preliminary interpretations, better time constraints are needed.

Evaporitic Unit 5 was attributed to the LGM, which corresponds to dry conditions in the region and which is a part of MIS 2. The subsequent lake-level rise, witnessed by the high-amplitude parallel stratified facies of Unit 6a, could thus represent the Bølling/Allerød (B/A) interstadial. The erosional unconformity at the top of Unit 6a represents a strong lake-level drop, probably corresponding to the onset of the Younger Dryas stadial (Fig. 14).

We relate the reconnection and the reinstallment of marine conditions to meltwater pulse MWP1b (Fig. 15), when rapid sea-level rise flooded the sill. The top reflector of Unit 6a can thus also be interpreted as a transgressive surface. Around the end of the Younger Dryas, just before reconnection with the Caribbean Sea, the shallow-water Unit 6b deposited. This was followed by the deeper-water, marine environment of Unit 6c.

Table 1
Standard deviation (SD) between sea/lake-level estimates before and after correction for total subsidence. Standard deviation is always smaller after correction.

Name	# of measurements	SD before correction	SD after correction	SD after/SD before
Unit 6b	4	1.59	1.24	0.78
Unit 6a	2	0.75	0.15	0.20
Unit 5	4	0.62	0.41	0.66
Unit 4c	1	0.00	0.00	-
Unit 4c	2	6.75	2.88	0.43
Unit 4c	5	1.16	1.06	0.91
Unit 4c	6	4.66	2.68	0.58
Unit 4c	3	6.19	1.84	0.30
Unit 4b	1	0.00	0.00	–
Unit 4b	7	4.10	1.67	0.41
Unit 4b	2	2.25	0.42	0.19
Unit 4a	4	5.51	2.83	0.51
Unit 4a	1	0.00	0.00	–
Unit 3	3	0.98	0.44	0.44
Unit 2c	1	0.00	0.00	–
Unit 2b	1	0.00	0.00	–
Unit 2b	2	3.56	1.48	0.42
Unit 2a	7	13.77	5.52	0.40
Unit 2a	4	12.04	4.40	0.37
Unit 1	3	5.45	0.07	0.01

5.6. Discussion of the assumptions

In this subchapter, we go back to and discuss the assumptions on which our reconstruction and interpretations are based. As a first approximation, sedimentation rate was considered constant through time in the centre of the Cerro Abajo Basin. Total subsidence was also assumed to be constant in time, although not in space.

Tuning the Gulf of Cariaco sea/lake level to global sea level led to adjustments of the sedimentation rates for each unit, which were previously considered as constant. Adjusted sedimentation rates (Fig. 14) vary in agreement with the changes of sedimentary environments. Highstand, open marine conditions are generally characterized by low sedimentation rates, and lacustrine conditions, with lower base level, by higher sedimentation rates. These variations in sedimentation rate thus corroborate the tuning to the eustatic curve. Units 5 and 6 deviate from this rule, but we attribute this to differences in compaction and overestimation of sound velocities in the upper, weakly compacted units. Considering a constant acoustic velocity of 1700 m/s for the sedimentary infill, the average sedimentation rate since the last interglacial is 0.84 mm/y. This is an acceptable sedimentation rate for this kind of environment and thereby supports our chronostratigraphy.

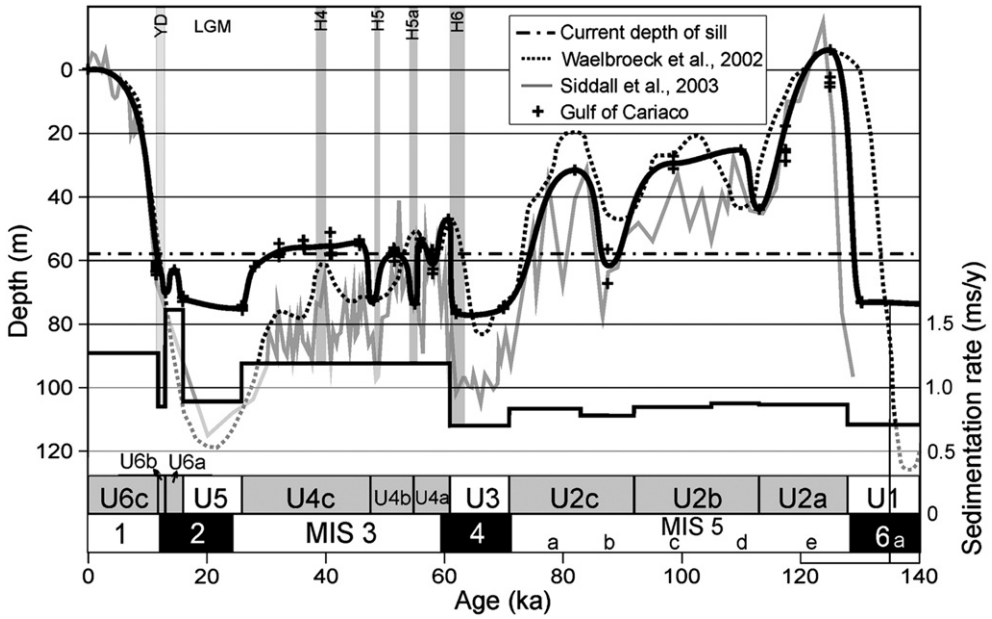

Fig. 14. Sea/lake-level curve of the Gulf of Cariaco tuned to the eustatic sea level curve (Siddall et al., 2003; Waelbroeck et al., 2002) and to Marine isotope Stages (MIS 2–MIS 4). Also Heinrich Events (HE) recorded in the Cariaco Basin (González et al., 2008; Hughen et al., 2004) are indicated (grey bars), since some unconformities could possibly be linked to some of them. However, the sea/lake-level curve of the Gulf of Cariaco has not been tuned to these HEs. To convert the base-level estimations from seconds to meters, a sound velocity of 1500 m/s for water and 1700 m/s for the sediments has been used (Hamilton, 1978).

After tuning to the eustatic sea-level curve, the activity through time of the faults in the area of the Cerro Abajo Basin can be estimated by measuring their vertical throw at each unit boundary. The difference in vertical throw only reflects the true activity of a fault if the vertical offset is in proportion to the total offset of the fault and if the activity is synsedimentary. We can assume this last condition to be fulfilled since the present-day vertical offsets of the seafloor are minimal (Figs. 3 and 4). This fault activity is a good proxy for the regional tectonic activity and consequently for tectonic subsidence. The component of total subsidence that is most likely to vary in time thus appears to have been constant during the considered time interval.

Estimations of sea level by using delta offlap breaks of the Manzanares and Casanay River systems give the same results. We can thereby conclude that the offlap breaks of either of the systems occur at approximately the same depth.

The erosional unconformities within Unit 4 have been attributed to a lowering of the lake level. However, it must be said that an intensification of tropical storm or hurricane activity—by a southern shift of the ITCZ—could lead to an increase in wave base depth, which could also generate such erosional unconformities. However, these southern shifts of the ITCZ, generally linked to Heinrich Events, were also accompanied by drier climate conditions in the region (González et al., 2008), and therefore this does not influence the main conclusions.

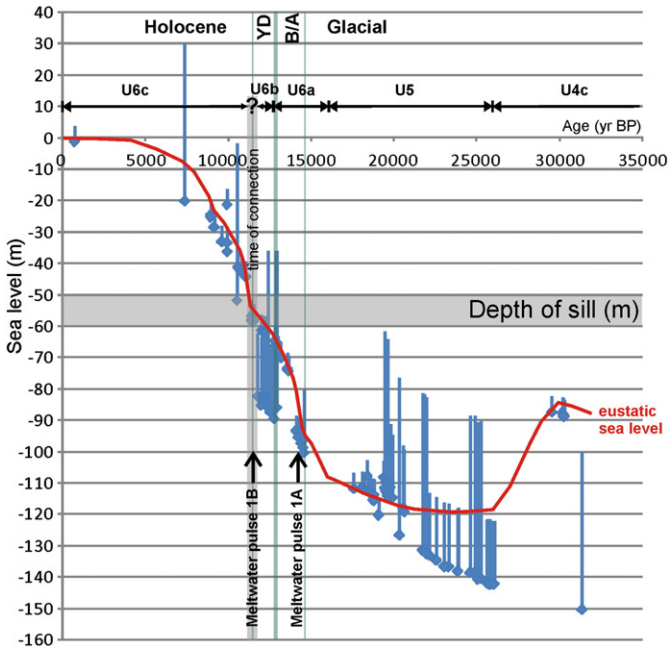

Fig. 15. Barbados sea level based on oxygen isotopes of foraminifera (data points in blue with vertical error bars depending on species, the red line is the derived sea level curve) (Peltier and Fairbanks, 2006) compared to Younger Dryas age in the Cariaco Basin (Hughen et al., 2004) and the Gulf of Cariaco sill depth (50–60 m). The last reconnection between the Gulf of Cariaco and the Cariaco Basin occurred just before or just after the end of the Younger Dryas. The Unit 6b fan deltas were formed during or just after the Younger Dryas, depending on the time of reconnection.

6. Conclusions

Seismic–stratigraphic interpretation of a dense grid of sparker reflection seismic profiles enabled us to reconstruct the history of sea/lake-level variations in the Gulf of Cariaco (NE Venezuela) during the last glacial–interglacial cycle.

- Three different sea/lake-level indicators were used for this reconstruction: i) evaporites, ii) delta offlap breaks, and iii) erosional unconformities.
- A simple subsidence model, based on a comparison of key reflectors with similar paleomorphology, was developed in order to correct for total subsidence. This subsidence model fits our observations that—on a regional scale—the central parts of the gulf are affected by higher subsidence rates than the more marginal parts. The tectonic activity, expressed by active faults, does not appear to significantly affect our subsidence model. Moreover, our data reveal that fault activity has been remarkably constant during the examined interval.

– The Gulf of Cariaco base-level curve has been tentatively tuned to the eustatic sea-level curves of Waelbroeck et al. (2002) and Siddall et al. (2003). The upper sedimentary infill of the gulf corresponds to the last glacial–interglacial cycle, starting from the end of MIS 6. During periods of connection, reconstructed sea level correlates well with eustatic sea level, both in terms of timing of variations and of their amplitude. During periods of disconnection, reconstructed lake levels can still be correlated to the stadials and interstadials. Some major Heinrich Events, as described by Hughen et al. (2004) and González et al. (2008), are possibly also recorded in the gulf's sedimentary infill. MIS 4, the LGM and the Younger Dryas were identified in the Gulf of Cariaco sedimentary record.

The Gulf of Cariaco thus holds a remarkably robust high-resolution record of regional variations in climate and lake level during MIS 2 to MIS 4 (glacial) and of sea level during periods of higher eustatic sea level (interglacials). There is a clear imprint of 5th-order climatic cycles in the sedimentary record. Stadials are recorded as (almost) complete desiccations, sometimes leading to the formation of an evaporite deposit (MIS 6, MIS 4 and LGM). The record of some possible marine incursions and imprints of HEs during MIS 3 could eventually lead to a better understanding of past changes in regional climate and global sea level.

The quality of this record and the vicinity to the iconic Cariaco Basin make the Gulf of Cariaco an ideal target for future ocean drilling (or long coring).

Acknowledgements

The Gulf of Cariaco survey is part of an overarching project entitled “Integrated investigations in sedimentology and seismo-tectonics for seismic hazards assessment along the south-Caribbean plate boundary”. This project is funded by the Venezuelan FONACIT through the Venezuelan Institute for Seismology FUNVISIS (PI-2003000090 and FONACIT-2002000478-Geodinos grants), and by the French CNRS/INSU (DYÉTI National Program and UMR 5025). The Université de Savoie also contributed to the project through a BQR/APS 2005/2006 grant. The Venezuelan–French cooperation grant ECOS-Norte VO4U01 (2004/2007) also helped to support our investigations by funding travels and stays of PhD students and senior researchers. We are very grateful to the whole crew of R/V GUAIQUERI II, led by Cpt. Sergio Valenzuela. Thanks to José Miguel Ramirez, Marcos Gutiérrez, Lisandro Gutiérrez, Ventura Hernández, Justino Alemán and Miguel Ángel Ramírez, for their hard work (night and day) and technical assistance. Thanks are also due to Wim Versteeg and Koen De Rycker of RCMG for acquisition of the seismic data. Maarten Van Daele and Jasper Moernaut are currently funded by the Flemish Fund for Scientific Research (FWO Vlaanderen). Finally, we thank D. Piper (editor-in-chief) and two anonymous reviewers for their constructive comments on an earlier version of this manuscript.

Appendix A. Supplementary data

Supplementary data to this article can be found online at doi:10.1016/j.margeo.2010.10.011.

References

Aksu, A.E., Hiscott, R.N., Yasar, D., Isler, F.I., Marsh, S., 2002. Seismic stratigraphy of Late Quaternary deposits from the southwestern Black Sea shelf: evidence for non-catastrophic variations in sea-level during the last similar to 10,000 yr. Marine Geology 190 (1–2), 61–94.

Anastasakis, G., Piper, D.J.W., Tziavos, C., 2007. Sedimentological response to neotectonics and sea-level change in a delta-fed, complex graben: Gulf of Amvrakikos, western Greece. Marine Geology 236 (1–2), 27–44.

Anderson, J.B., Rodriguez, A., Abdulah, K.C., Fillon, R.H., Banfield, L.A., McKeown, H.A., Wellner, J.S., 2004. Late Quaternary Stratigraphic evolution of the northern Gulf of Mexico margin: a synthesis. In: Anderson, J.B., Fillon, R.H. (Eds.), Late Quaternary Stratigraphic evolution of the northern Gulf of Mexico margin: Society for Sedimentary Geology, Tulsa, Okla, pp. 1–23.

Anselmetti, F.S., Ariztegui, D., Hodell, D.A., Hillesheim, M.B., Brenner, M., Gilli, A., McKenzie, J.A., Mueller, A.D., 2006. Late Quaternary climate-induced lake level variations in Lake Petén Itzá, Guatemala, inferred from seismic stratigraphic analysis. Palaeogeography, Palaeoclimatology, Palaeoecology 230 (1–2), 52–69.

Anselmetti, F.S., Ariztegui, D., De Batist, M., Gebhardt, A.C., Haberzettl, T., Niessen, F., Ohlendorf, C., Zolitschka, B., 2009. Environmental history of southern Patagonia unravelled by the seismic stratigraphy of Laguna Potrok Aike. Sedimentology 56 (4), 873–892.

Antonius, A., 1980. Occurrence and distribution of stony corals in the Gulf of Cariaco, Venezuela. Internationale Revue der Gesamten Hydrobiologie 65 (3), 321–338.

Ascanio, G., 1972. Geología de los Cerros de Caigüire, Cumaná, Estado Sucre. IV Congreso Geológico Venezolano, pp. 1279–1288.

Audemard, F.A., 2000. Major Active Faults of Venezuela. 31st International Geological Congress, Río de Janeiro, Brasil, p. 4.

Audemard, F.A., 2006. Surface rupture of the Cariaco July 09, 1997 earthquake on the El Pilar fault, northeastern Venezuela. Tectonophysics 424 (1–2), 19–39.

Audemard, F.A., 2007. Revised seismic history of the El Pilar fault, Northeastern Venezuela, from the Cariaco 1997 earthquake and recent preliminary paleoseismic results. Journal of Seismology 11 (3), 311–326.

Audemard, F.A., Machette, M., Cox, J., Hart, R., Haller, K., 2000. Map of Quaternary Faults of Venezuela. Scale 1:2.000.000, International Lithosphere Program Task Group II-2: major active faults of the world (Regional Coord.: Carlos Costa, Univ. San Luis-Argentina; ILP II-2 co-chairman Western Hemisphere: Michael Machette, USGS-Colorado). USGS. Reprinted as a XXX FUNVISIS Anniversary special edition. pp.

Audemard, F., Beck, C., Moernaut, J., De Rycker, K., De Batist, M., Sanchez, J., Gonzalez, M., Sanchez, C., Versteeg, W., Malave, G., Schmitz, M., Van Welden, A., Carrillo, E., Lemus, A., 2007. The underwater depression of Guaracayal, estado Sucre, Venezuela: a barrier to the propagation of the coseismic break along the El Pilar Fault. Interciencia 32 (11), 735–741.

Baumbach, M., Grosser, H., Torres, G.R., Gonzales, J.L.R., Sobiesiak, M., Welle, W., 2004. Aftershock pattern of the July 9, 1997 Mw = 6.9 Cariaco earthquake in Northeastern Venezuela. Tectonophysics 379 (1–4), 1–23.

Beck, C., Mercier de Lepinay, B., Schneider, J.L., Cremer, M., Cagatay, N., Wendenbaum, E., Boutareaud, S., Menot, G., Schmidt, S., Weber, O., Eris, K., Armijo, R., Meyer, B., Pondard, N., Gutscher, M.A., 2007. Late Quaternary co-seismic sedimentation in the Sea of Marmara's deep basins. Sedimentary Geology 199 (1–2), 65–89.

Bellizzia, A., Pimentel, N., Bajo de Osuna, R., 1976. Mapa geológico-estructural de Venezuela. Scale 1: 500,000. Ministerio de Minas e Hidrocarburos.—Ed. Foninves, Caracas.

Ben-Avraham, Zoback, 1992. Transform-normal and asymmetric basins—an alternative to pull-apart models. Geology 20 (5), 423–426.

Bertoni, C., Cartwright, J.A., 2007. Major erosion at the end of the Messinian Salinity Crisis: evidence from the Levant Basin, Eastern Mediterranean. Basin Research 19 (1), 1–18.

Bonilla, J., Quintero, A., Álvarez, M., De Grado, A., Gil, H., Guevara, M., Martínez, G., Saint, S., 1998. Condición ambiental de la ensenada Grande del Obispo, Estado Sucre, Venezuela. Scientia 13, 35–59.

Campos, V., 1981. Une transversale de la Chaîne Caraïbe et de la marge vénézuélienne dans le secteur de Carúpano (Vénézuela oriental): structure géologique et évolution géodynamique. Western Bretagne University, Brest. 160 pp.

Caraballo, L.F., 1982a. El Golfo de Cariaco. Parte I: Morfología y batimetría submarina. Estructuras y tectonismo reciente. Boletín del Instituto Oceanográfico, Universidad de Oriente 21 (1-2), 13–35.

Caraballo, L.F., 1982b. El golfo de Cariaco. Parte II: Los sedimentos superficiales y su distribución por el fondo. Fuente de sedimentos. Análisis mineralógico. Boletín del Instituto Oceanográfico, Universidad de Oriente 21 (1-2), 37–65.

Chappell, J., Shackleton, N.J., 1986. Oxygen isotopes and sea-level. Nature 324 (6093), 137–140.

Chiang, J.C.H., Kushnir, Y., Giannini, A., 2002. Deconstructing Atlantic Intertropical Convergence Zone variability: influence of the local cross-equatorial sea surface temperature gradient and remote forcing from the eastern equatorial Pacific. Journal of Geophysical Research-Atmospheres 107 (D1-D2), 1–19.

D'Agostino, K., Seltzer, G., Baker, P., Fritz, S., Dunbar, R., 2002. Late-Quaternary lowstands of Lake Titicaca: evidence from high-resolution seismic data. Palaeogeography, Palaeoclimatology, Palaeoecology 179 (1–2), 97–111.

Escalona, A., Mann, P., Jaimes, M., 2011. Miocene to recent Cariaco basin, Offshore Venezuela: Structure, tectonosequences and basin-forming mechanisms. Marine and Petroleum Geology 28 (1), 177–199.

Galloway, W.E., 1975. Process framework for describing the morphologic and stratigraphic evolution of deltaic depositional systems. In: Broussard, M.L. (Ed.), Deltas, models for exploration: Houston Geological Society Houston, pp. 87–98.

Gardner, J.V., Calder, B.R., Clarke, J.E.H., Mayer, L.A., Elston, G., Rzhanov, Y., 2007. Drowned shelf-edge deltas, barrier islands and related features along the outer continental shelf north of the head of De Soto Canyon, NE Gulf of Mexico. Geomorphology 89 (3–4), 370–390.

Gilbert, G.K., 1885. The topographic features of lake shores. United States Geological Survey Annual Report, pp. 69–123.

González, C., Dupont, L.M., Behling, H., Wefer, G., 2008. Neotropical vegetation response to rapid climate changes during the last glacial period: palynological evidence from the Cariaco Basin. Quaternary Research 69 (2), 217–230.

Hackley, P.C., Urbani, F., Karlsen, A.W., Garrity, C.P., 2005. Geologic shaded relief map of Venezuela, Open-File Report—U. S. Geological Survey, 2005. U. S. Geological Survey, Reston, VA, United States.

Håkanson, L., Jansson, M., 1983. Principles of Lake Sedimentology. The Blackburn Press. 316 pp.

Hamilton, E.L., 1978. Sound velocity–density relations in sea-floor sediments and rocks. The journal of the Acoustical Society of America 63 (2), 366–377.
Haug, G.H., Hughen, K.A., Sigman, D.M., Peterson, L.C., Rohl, U., 2001. Southward migration of the intertropical convergence zone through the Holocene. Science 293 (5533), 1304–1308.
Hearty, P.J., Neumann, A.C., O'Leary, M.J., 2007. Comment on "Record of MIS 5 sea-level highstands based on U/Th dated coral terraces of Haiti" by Dumas et al. [Quaternary International 2006 106–118]. Quaternary International 162-163, 205–208.
Hughen, K.A., Southon, J.R., Lehman, S.J., Overpeck, J.T., 2000. Synchronous radiocarbon and climate shifts during the last deglaciation. Science 290 (5498), 1951–1954.
Hughen, K.A., Eglinton, T.I., Xu, L., Makou, M., 2004. Abrupt tropical vegetation response to rapid climate changes. Science 304 (5679), 1955–1959.
Hughen, K., Southon, J., Lehman, S., Bertrand, C., Turnbull, J., 2006. Marine-derived C-14 calibration and activity record for the past 50,000 years updated from the Cariaco Basin. Quaternary Science Reviews 25 (23–24), 3216–3227.
Imbrie, J., Boyle, E.A., Clemens, S.C., Duffy, A., Howard, W.R., Kukla, G., Kutzbach, J., Martinson, D.G., McIntyre, A., Mix, A.C., Molfino, B., Morley, J.J., Peterson, L.C., Pisias, N.G., Prell, W.L., Raymo, M.E., Shackleton, N.J., Toggweiler, J.R., 1992. On the structure and origin of major glaciation cycles. 1. Linear responses to Milankovitch forcing. Paleoceanography 7 (6), 701–738.
Jouet, G., Berne, S., Rabineau, M., Bassetti, M.A., Bernier, P., Dennielou, B., Sierro, F.J., Flores, J.A., Taviani, M., 2006. Shoreface migrations at the shelf edge and sea-level changes around the Last Glacial Maximum (Gulf of Lions, NW Mediterranean). Marine Geology 234 (1–4), 21–42.
Kendall, A.C., Harwood, G.M., 1996. Marine evaporites: arid shorelines and basins. In: Reading, H.G. (Ed.), Sedimentary environments: processes, facies, and stratigraphy, pp. 283–324.
Larcombe, P., Carter, R.M., 1998. Sequence architecture during the Holocene transgression: an example from the Great Barrier Reef shelf, Australia. Sedimentary Geology 117 (1–2), 97–121.
Le Pichon, X., Sengör, A., Demirbag, E., Rangin, C., Imren, C., Armijo, R., Görür, N., Çagatay, N., Mercier de Lepinay, B., Meyer, B., 2001. The active Main Marmara Fault. Earth and Planetary Science Letters 192 (4), 595–616.
Lea, D.W., Pak, D.K., Peterson, L.C., Hughen, K.A., 2003. Synchroneity of tropical and high-latitude Atlantic temperatures over the last glacial termination. Science 301 (5638), 1361–1364.
Leyden, B.W., 1985. Late Quaternary aridity and Holocene moisture fluctuations in the Lake Valencia Basin, Venezuela. Ecology 66 (4), 1279–1295.
Liquete, C., Canals, M., De Mol, B., De Batist, M., Trincardi, F., 2008. Quaternary stratal architecture of the Barcelona prodeltaic continental shelf (NW Mediterranean). Marine Geology 250 (3–4), 234–250.
Macsotay, O., 1976. Bioestratigrafía de algunas secciones pleistocenas del nororiente de Venezuela. Boletín de Geología, Caracas, Publ. Esp. 7 (2), 985–996.
Macsotay, O., 1977. Observaciones sobre el neotectonismo Cuaternario en el nororiente Venezolano. Boletín de Geología, Caracas, Publ. Esp. 7 (3), 1861–1883.
Makou, M.C., Hughen, K.A., Xu, L., Sylva, S.P., Eglinton, T.I., 2007. Isotopic records of tropical vegetation and climate change from terrestrial vascular plant biomarkers preserved in Cariaco Basin sediments. Organic Geochemistry 38 (10), 1680–1691.
McGlue, M.M., Lezzar, K.E., Cohen, A.S., Russell, J.M., Tiercelin, J.J., Felton, A.A., Mbede, E., Nkotagu, H.H., 2008. Seismic records of late Pleistocene aridity in Lake Tanganyika, tropical East Africa. Journal of Paleolimnology 40 (2), 635–653.
Minster, J., Jordan, T., 1978. Present-day plate motions. Journal of Geophysical Research-Atmospheres 83, 5331–5354.
Moernaut, J., Verschuren, D., Charlet, F., Kristen, I., Fagot, M., De Batist, M., 2010. The seismic–stratigraphic record of lake-level fluctuations in Lake Challa: hydrological stability and change in equatorial East Africa over the last 140 kyr. Earth and Planetary Science Letters 290 (1–2), 214–223.
Molnar, P., Sykes, L., 1969. Tectonics of the Caribbean and Middle America Regions from focal mechanisms and seismicity. Geological Society of America Bulletin 80, 1639–1684.
Nurmi, R.D., 1988. Geologic interpretation of well logs and seismic measurements in reservoirs associated with evaporites. In: Schreiber, B.C. (Ed.), Evaporites and hydrocarbons. Columbia University Press, New York, pp. 405–459.
Paige, S., 1930. The Earthquake at Cumaná, Venezuela. January 17, 1929. Bulletin of the Seismological Society of America 20 (12), 1–10.
Peltier, W.R., Fairbanks, R.G., 2006. Global glacial ice volume and Last Glacial Maximum duration from an extended Barbados sea level record. Quaternary Science Reviews 25 (23–24), 3322–3337.
Perez, O.J., Bilham, R., Bendick, R., Hernandez, N., Hoyer, M., Velandia, J.R., Moncayo, C., Kozuch, M., 2001. Relative velocity between the Caribbean and South American plates from GPS observations in northern Venezuela. Interciencia 26 (2), 69–74.
Peterson, L.C., Haug, G.H., 2006. Variability in the mean latitude of the Atlantic Intertropical Convergence Zone as recorded by riverine input of sediments to the Cariaco Basin (Venezuela). Palaeogeography, Palaeoclimatology, Palaeoecology 234 (1), 97–113.
Peterson, L.C., Haug, G.H., Hughen, K.A., Rohl, U., 2000a. Rapid changes in the hydrologic cycle of the tropical Atlantic during the last glacial. Science 290 (5498), 1947–1951.
Peterson, L.C., Haug, G.H., Murray, R.W., Yarincik, K.M., King, J.W., Bralower, T.J., Kameo, K., Rutherford, S.D., Pearce, R.B., 2000b. Late Quaternary stratigraphy and sedimentation at Site 1002, Cariaco Basin (Venezuela). In: Leckie, R.M., Sigurdsson, H., Acton, G.D., Draper, G. (Eds.), Proceedings of the Ocean Drilling Program, Scientific Results, pp. 85–99.
Piper, D.J.W., Aksu, A.E., 1992. Architecture of stacked quaternary deltas correlated with global oxygen isotopic curve. Geology 20 (5), 415–418.
Postma, G., 1990. Depositional architecture and facies of river and fan deltas: a synthesis. In: Colella, A., Prior, D.B. (Eds.), Coarse-grained deltas: Special Publications Number 10 of the International Association of Sedimentologists, pp. 13–27.
Quintero, A., Caraballo, L.F., Bonilla, J., Terejova, G., Rivadula, R., 2006. Sedimentos marino costeros del Golfo de Cariaco, Venezuela. Boletín del Instituto Oceanográfico Venezuela, Universidad de Oriente 45 (2), 127–139.
Rabineau, M., Berné, S., Aslanian, D., Olivet, J.-L., Joseph, P., Guillocheau, F., Bourillet, J.-F., Ledrezen, E., Granjeon, D., 2005. Sedimentary sequences in the Gulf of Lion: a record of 100,000 years climatic cycles. Marine and Petroleum Geology 22 (6–7), 775–804.
Rabineau, M., Berné, S., Olivet, J.-L., Aslanian, D., Guillocheau, F., Joseph, P., 2006. Paleo sea levels reconsidered from direct observation of paleoshoreline position during Glacial Maxima (for the last 500,000 yr). Earth and Planetary Science Letters 252 (1–2), 119–137.
Reading, H.G., 1996. Sedimentary environments: processes, facies, and stratigraphy. Blackwell Science. 688 pp.
Rod, E., 1956. Strike-slip faults of northern Venezuela. American Association of Petroleum Geologists Bulletin 40, 457–476.
Rull, V., 1996. Late Pleistocene and Holocene climates of Venezuela. Quaternary International 31, 85–94.
Rull, V., 1999. Palaeoclimatology and sea-level history in Venezuela. New data, land–sea correlations, and proposals for future studies in the framework of the IGBP-pages project. Interciencia 24 (2), 92–101.
Schmitz, M., Romero, R., Bonvive, F., Audemard, F.A., González, J., 2006. Resultados de mediciones sísmicas e implicaciones de dinámica de suelo en torno al Hospital Dr. Antonio Patricio de Alcalá, Cumaná, Estado Sucre, Venezuela. IMME 44, 30–50.
Siddall, M., Rohling, E.J., Almogi-Labin, A., Hemleben, C., Meischner, D., Schmelzer, I., Smeed, D.A., 2003. Sea-level fluctuations during the last glacial cycle. Nature 423 (6942), 853–858.
Skene, K.I., Piper, D.J.W., Aksu, A.E., Syvitski, J.P.M., 1998. Evaluation of the global oxygen isotope curve as a proxy for quaternary sea-level by modeling of delta progradation. Journal of Sedimentary Research 68 (6), 1077–1092.
Smith, I.R., Sinclair, I.J., 1972. Deep water waves in lakes. Freshwater Biol 2, 387–399.
Stéphan, J.-F., Beck, C., Bellizzia, A., Blanchet, R., 1980. La Chaîne Caraïbe du Pacifique à l'Atlantique. XXVIth International Geological Congress, Paris, pp. 38–59.
Sylvester, A.G., 1988. Strike-slip faults. Geological Society of America Bulletin 100, 1666–1703.
Thunell, R., Tappa, E., Varela, R., Llano, M., Astor, Y., Muller-Karger, F., Bohrer, R., 1999. Increased marine sediment suspension and fluxes following an earthquake. Nature 398 (6724), 233–236.
Urabe, A., Tateishi, M., Inouchi, Y., Matsuoka, H., Inoue, T., Dmytriev, A., Khlystov, O.M., 2004. Lake-level changes during the past 100,000 years at Lake Baikal, southern Siberia. Quaternary Research 62 (2), 214–222.
Vierbuchen, R.C., 1978. Geology of the El Pilar Fault region, State of Sucre, and its tectonic implications. University of Princeton. 169 pp.
Vierbuchen, R.C., 1984. The geology of the El Pilar Fault zone and adjacent areas in northeastern Venezuela. Geological Society of America Bulletin, Memoir 162, 189–212.
Vignali, M., 1977. Geology between Casanay and El Pilar (El Pilar Fault zone), Estado Sucre, Venezuela. VIIIth Caribb. Geol. Conf., Curaçao, pp. 215–216.
Waelbroeck, C., Labeyrie, L., Michel, E., Duplessy, J.C., McManus, J.F., Lambeck, K., Balbon, E., Labracherie, M., 2002. Sea-level and deep water temperature changes derived from benthic foraminifera isotopic records. Quaternary Science Reviews 21 (1–3), 295–305.
Weber, J.C., Dixon, T.H., DeMets, C., Ambeh, W.B., Jansma, P., Mattioli, G., Saleh, J., Sella, G., Bilham, R., Perez, O., 2001. GPS estimate of relative motion between the Caribbean and South American plates, and geologic implications for Trinidad and Venezuela. Geology 29 (1), 75–78.
Weller, J.M., 1960. Stratigraphic Principles and Practice. Harper, New York. 725 pp.
Yarincik, K.M., Murray, R.W., Peterson, L.C., 2000. Climatically sensitive eolian and hemipelagic deposition in the Cariaco Basin, Venezuela, over the past 578,000 years: results from Al/Ti and K/Al. Paleoceanography 15 (2), 210–228.